Article

Synthesis of Structurally Related Coumarin Derivatives as Antiproliferative Agents

Ezequiel F. Bruna-Haupt,* Marcelle D. Perretti, Hugo A. Garro, Romen Carrillo, Félix Machín,
Isabel Lorenzo-Castrillejo, Lucas Gutiérrez, Esteban G. Vega-Hissi, Macarena Mamberto,
Mauricio Menacho-Marquez, Claudio O. Fernández, Celina García, and Carlos R. Pungitore

Cite This: https://doi.org/10.1021/acsomega.3c03181

Read Online

| ACCESS | | Metrics & More | | Article Recommendations | | SI Supporting Information |

ABSTRACT: A library of structurally related coumarins was generated through synthesis reactions and chemical modification reactions to obtain derivatives with antiproliferative activity both *in vivo* and *in vitro*. Out of a total of 35 structurally related coumarin derivatives, seven of them showed inhibitory activity in *in vitro* tests against *Taq* DNA polymerase with IC_{50} values lower than 250 μM. The derivatives 4-(chloromethyl)-5,7-dihydroxy-*2H*-chromen-2-one (**2d**) and 4-((acetylthio)methyl)-2-oxo-*2H*-chromen-7-yl acetate (**3c**) showed the most promising anti-polymerase activity with IC_{50} values of 20.7 $\pm$ 2.10 and 48.25 $\pm$ 1.20 μM, respectively. Assays with tumor cell lines (HEK 293 and HCT-116) were carried out, and the derivative 4-(chloromethyl)-7,8-dihydroxy-*2H*-chromen-2-one (**2c**) was the most promising, with an IC_{50} value of 8.47 μM and a selectivity index of 1.87. In addition, the derivatives were evaluated against *Saccharomyces cerevisiae* strains that report about common modes of actions, including DNA damage, that are expected for agents that cause replicative stress. The coumarin derivatives 7-(2-(oxiran-2-yl)ethoxy)-*2H*-chromen-2-one (**5b**) and 7-(3-(oxiran-2-yl)propoxy)-*2H*-chromen-2-one (**5c**) caused DNA damage in *S. cerevisiae*. The *O*-alkenylepoxy group stands out as that with the most important functionality within this family of 35 derivatives, presenting a very good profile as an antiproliferative scaffold. Finally, the *in vitro* antiretroviral capacity was tested through RT-PCR assays. Derivative **5c** showed inhibitory activity below 150 μM with an IC_{50} value of 134.22 $\pm$ 2.37 μM, highlighting the *O*-butylepoxy group as the functionalization responsible for the activity.
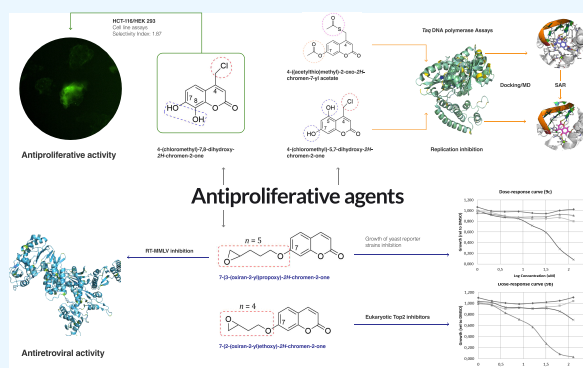
1. INTRODUCTION

Hyperproliferative diseases, such as cancer and autoimmune conditions, are characterized by uncontrolled DNA replication.[1] DNA replication is a fundamental process for the proliferation and survival of living organisms, which is catalyzed by enzymes known as DNA polymerases (Pol).[2] Pol inhibitors could therefore be employed as anticancer chemotherapy agents because they inhibit cell proliferation.[3]

Many advances have been made in controlling the spread and proliferation of metastatic cancers; however, research on drug resistance and side effects of different drugs in biomedical sciences remains an imperative need.[4] Heterocyclic oxygenated compounds like coumarins (2H-1-benzopyran-2-one) and their derivatives represent an important class of natural products with several biological activities and ubiquitous in nature.[5]

The pharmacological activities of coumarin can be attributed to its unique chemical structure, which allows for non-covalent interactions such as $\pi-\pi$ stacking, hydrophobic interactions, electrostatic interactions, hydrogen bonding, metal coordina-tion, and van der Waals forces with various active sites in organisms.[6,7]

Small modifications in the coumarin structure and the introduction of diverse functional groups have allowed researchers to synthesize more complex and diverse coumarin derivatives with a great application value and performance.[1] These characteristics make coumarin a distinctive heterocyclic group in the field of pharmacochemistry.[2]

Coumarin, of both natural and synthetic origins, displays versatile pharmacological properties that include antimicrobial, antioxidant, anticoagulant, anti-Alzheimer, anti-HIV, and anticancer activities.[8] Since the 1960s, coumarin and its derivatives have shown an extremely wide and significant potential in the field of antitumor therapy.[9,10] The mechanisms

A

A)

B)
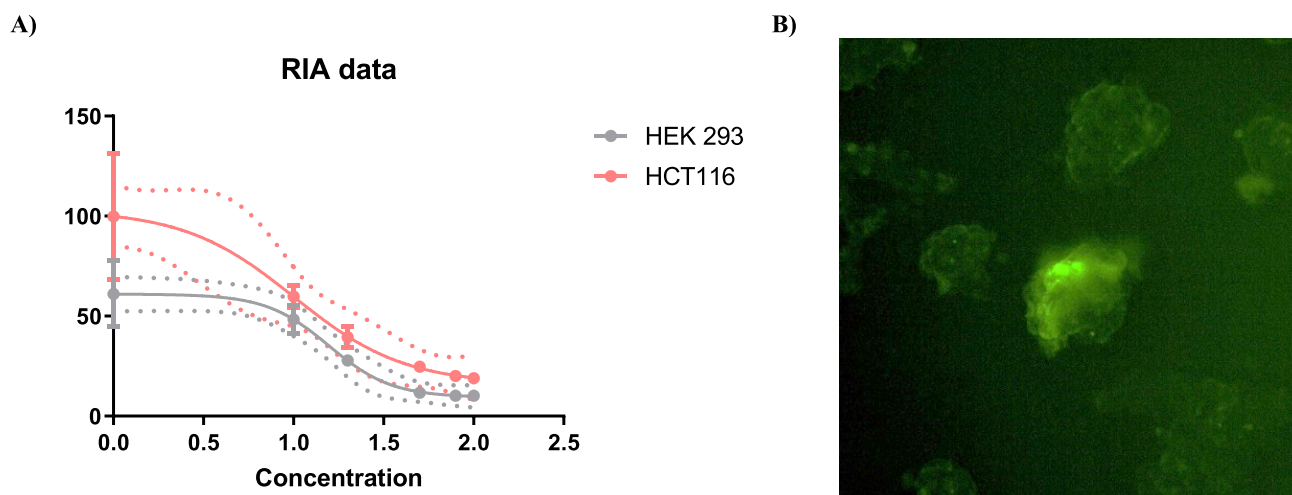
Figure 1. (A) Cytotoxic effects against human colorectal cancer cell lines HCT-116 and HEK 293. (B) Internalization of **2c** within the cells, monitored by fluorescence microscopy.

behind their antitumor activity can be diverse, including carbonic anhydrase inhibition, PI3K/Akt/mTOR signaling pathway targeting, multiple drug resistance inhibition, apoptosis induction, telomerase inhibition, and the inhibition of a wide range of DNA-related enzymes (polymerases, topoisomerases, etc.).[1,5] An example of this are typical naturally occurring coumarins, like esculetin (6,7-dihydroxycoumarin) and scopoletin (6-methoxy-7-hydrocoumarin), among others, which have exhibited promising activity in several carcinoma cell lines.[2,11] A six-coumarin series (mansorin-A, mansorin-B, mansorin-C, mansorin-I, mansorin-II, and mansorin-III) isolated from the heartwood of the *Mansonia gagei* family Sterculariaceae exhibited cytotoxic effects via a telomerase enzyme inhibitory effect, protein kinase inhibition, and oncogene downregulation.[12] Also, coumarin derivatives isolated from the *Pterocaulon* genus (Asteraceae) have exhibited promising activity against myeloid murine leukemia virus-reverse transcriptase (MMLV-RT) and *Taq* DNA polymerase.[13]

On the other hand, a large amount of synthetic coumarin derivatives have shown a broad spectrum of antitumor actions through the interaction over different cellular pathways, for instance, 6-methylcoumarin coupled with TPP-induced HeLa cell apoptosis by promoting ROS generation,[14] and coumarin-linked 6-methylpyridine and hybrids of 1,2,3-triazole and 4-substituted coumarin have shown an induction of G2/M phase cell cycle arrest in *in vivo* assays.[7,9,15] Moreover, some of them such as Irosustat are under clinical trials for the treatment of various cancers, suggesting that coumarin is a highly privileged scaffold for the development of novel anticancer drugs.[8]

A new coumarin-based non-nucleoside reverse transcriptase inhibitor (NNRTI) is currently under clinical evaluations for the treatment of HIV-infected individuals. Therefore, coumarin derivatives represent attractive scaffolds for the design and development of novel anti-HIV drugs.[16]

In previous articles, we described the design, synthesis, and *in vitro* antitumor profile of hydroxylated coumarin nuclei and derivatives containing a side chain with the presence of terminal and intermediate olefins (Figure 1). These studies revealed an interesting activity, in particular the ability to induce antiproliferative effects and apoptosis in tumor cell lines. These cellular properties were related to the presence of

the double bond in the side chain, which seemed to be a key feature in promoting antitumor activity.[17]

Continuing our studies in this field, to enhance the inhibitory activity against DNA-related enzymes of our compounds, as well as to increase their potency, we synthesized a new collection of derivatives capable of increasing such activity and endowed with intrinsic cytotoxicity. The different substituents used were selected on the basis of previously obtained results, in particular showing epoxy scaffold derivatives on *O*-alkenylcoumarins, as it yielded more promising results in the previous series of compounds.[14,17]

2. RESULTS AND DISCUSSION

2.1. Chemistry. The structurally related coumarin derivatives were synthesized using different chemical modification reactions using concepts of molecular simplification and chemical synthesis reactions (Schemes 1 to 5). The

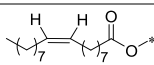**Scheme 1. Commercial 7-Hydroxycoumarin (Numbered Core) Esterified with Fatty Acids**
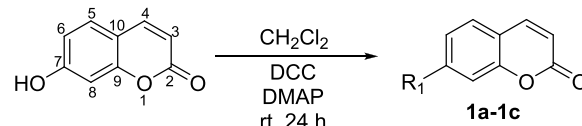
detailed procedures for each reaction are described in the Materials and Methods section. All final derivatives were characterized using ^{1}H NMR, ^{13}C NMR, and mass spectrometry (see the Supporting Information).

To further enhance the activity of the compounds, we continued our effort with the modifications at the side chain position of hydroxycoumarins. Coumarin derivatives **1** were synthesized according to the protocol outlined in Scheme 1, starting from esterification reactions of 7-hydroxycoumarin with long-chain fatty acids such as palmitic, stearic, and oleic acid (Table 1).

By using simple von Pechmann synthesis between phenolic reagents and β-ketoesters has proven to be an efficient alternative method for obtaining oxygenated coumarin cores **2** (Scheme 2) incorporating into the derivatives obtained in

Table 1. Half-Maximal Inhibitory Concentration IC$_{50}$ against *Taq* DNA Polymerase for Compounds 1

Compound	R$_1$	Pol IC$_{50}$ Values[a] (μM)
1a		113.46 ± 4.18
1b		>200
1c		>200

[a]IC$_{50}$ values were determined by interpolation from plots and enzyme activity vs inhibitor concentration. The IC$_{50}$ values are the means from at least three independent experiments (*n* = 3). Inactive at 200 μM (highest concentration tested).

this series of key functional groups for the generation of interactions with molecular targets.

Once these structures were generated, derivatives **3** were obtained through the conventional chemical modifications of some of compounds **2** (through ether, ester, and thioester incorporation) (Scheme 2 and Table 2) to diversify the active functional groups positioned on the coumarin scaffold and thus improve the chances of interactions with the molecular target.

In addition, three *O*-alkenylcoumarins already tested against *Taq* DNA polymerase (compounds **4**) in previous investigations were obtained[17] to evaluate their retroviral antiproliferative activity in biological assays against the RT M-MLV enzyme and, moreover, test its antiproliferative capacity at the level of Top2 inhibition in tests with *Saccharomyces cerevisiae* reporter strains as a cellular model (Scheme 3 and Table 3).

Using simple *m*CPBA epoxidation of *O*-alkenylcoumarins mentioned above, compounds **5** (Scheme 3) were obtained, highlighting the introduction of highly reactive terminal epoxide groups to improve the results obtained in previous works for derivatives **4**. According to our knowledge, compounds **5a** and **5c** are new and have not been previously described in the literature.

It is well known that alkyl coumarins have shown interesting antiproliferative and antiviral effects;[18,19] wherefore, compounds **6** were obtained from chemical modification reactions using the Williamson synthesis for the ether formation. For this, 7-hydroxycoumarin (commercial reagent) and compound **2e** (Scheme 4 and Table 4) were used in the presence of different alkyl halides.

Molecular hybrids have been of great interest for the expansion of spectra of biological activities. Coumarin-glycoside structures have shown great progress in the development of new antiproliferative scaffolds.[20,21]

To provide dual molecules for possible enzymatic bimodal recognitions, an interesting series of coumarin-glycoside

Scheme 2. Functionalized Coumarin Obtained Using Von Pechmann Synthesis
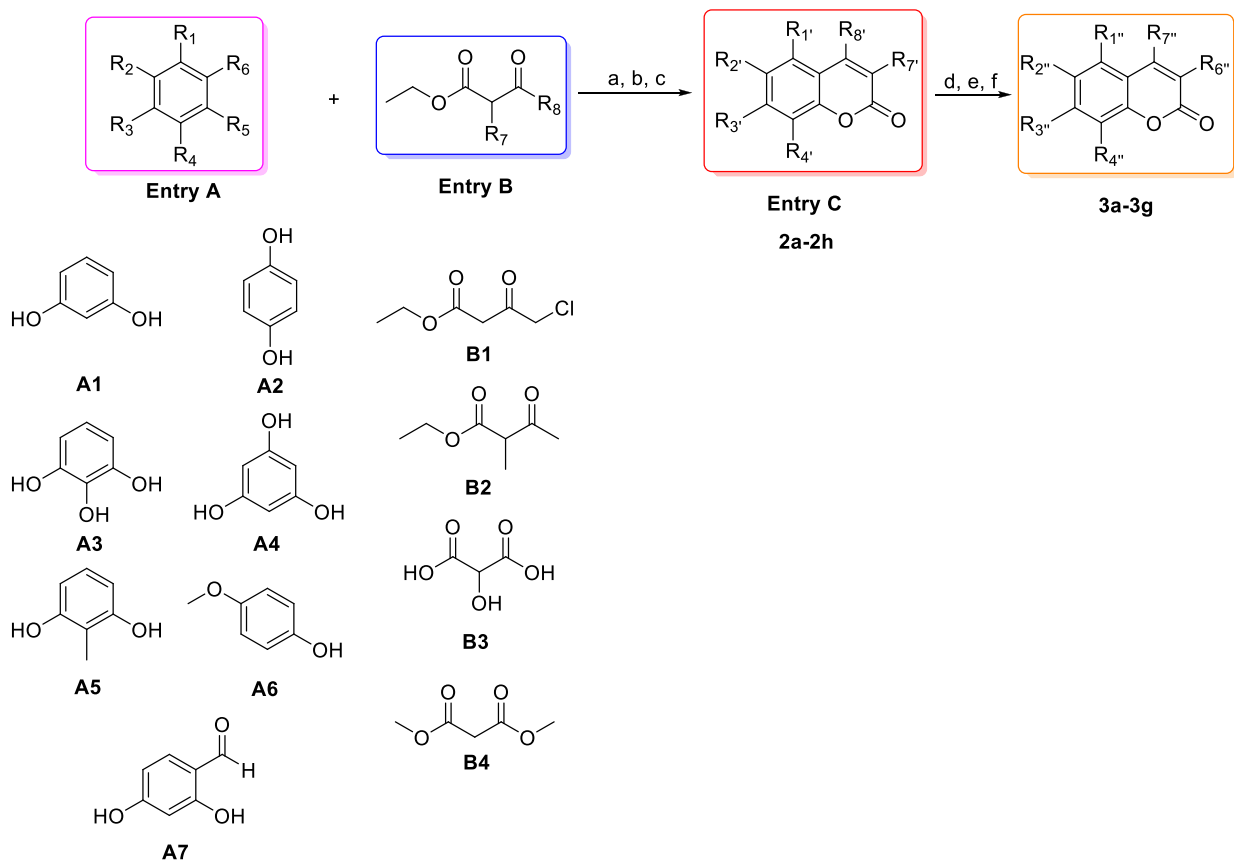
[a][a]HClO$_4$, 85 °C, 6 h; [b]H$_2$SO$_4$, 120 °C, 6 h; [c]methanol, piperidine, reflux 12 h. [d]NBS, AIBN, DCA, reflux 6 h; [e]CaCO$_3$, H$_2$O, dioxane, 80 °C, 24 h; [f]THF, thioacetic acid, DIPEA, rt, 12 h.

Table 2. Oxygenated Coumarins Obtained through Von Pechmann Synthesis (2a–2h) and Chemical Modification on Oxygenated Coumarin Cores (3a–3g) and Inhibition of *Taq* DNA Polymerase and Cell Line Assays

Compound	$R_{1'}$	$R_{2'}$	$R_{3'}$	$R_{4'}$	$R_{7'}$	$R_{8'}$	Entry A	Entry B	Pol IC_{50} Values[g]	IC_{50} Cell Lines HEK293[h]	HCT-116[h]	SI[i]
[a]2a	H	H	*−OH	H	H	CH2Cl	A1	B1	>200	15.85[a]	8.47[a]	1.87
[a]2b	H	*−OH	H	H	H	CH2Cl	A2	B1	>200	>20	>20	-
[a]2c	H	H	*−OH	*−OH	H	CH2Cl	A3	B1	142.0 ± 3.40	>20	>20	-
[a]2d	*−OH	H	*−OH	H	H	CH2Cl	A4	B1	20.7 ± 2.10	>20	>20	-
[a]2e	*−OH	H	*−OH	H	*−CH3	*−CH3	A4	B2	>200	>20	>20	-
[b]2f	H	H	*−OH	*−CH3	H	H	A5	B3	>200	>20	>20	-
[a]2g	H	H3C−O−*	H	H	H	CH2Cl	A6	B1	>200	>20	>20	-
[c]2h	H	H	*−OH	H	C(=O)O−methyl	H	A7	B4	129.08 ± 2.50	>20	>20	-

Compound	$R_{1''}$	$R_{2''}$	$R_{3''}$	$R_{4''}$	$R_{6''}$	$R_{7''}$	Entry C				
[d]3a	H	H	acetyl−O−*	*CH2Br	H	H	2f	>200	>20	>20	-
[e]3b	H	H	*−OH	*CH2OH	H	H	3a	>200	>20	>20	-
[f]3c	H	H	acetyl−O−*	H	H	thioester C(=O)S−CH2*	2a	48.25 ± 1.20	>20	>20	-
[f]3d	H	H	*−OH	H	H	thioester C(=O)S−CH2*	2a	143.25 ± 4.22	>20	>20	-
[f]3e	H	*−OH	H	H	H	thioester C(=O)S−CH2*	2b	188.35 ± 19.40	>20	>20	-
[f]3f	H	H3C−O−*	H	H	H	thioester C(=O)S−CH2*	2g	>200	>20	>20	-
[f]3g	H	acetyl−O−*	H	H	H	thioester C(=O)S−CH2*	2b	>200	>20	>20	-

[a]HClO4, 85 °C, 6 h. [b]H2SO4, 120 °C, 6 h. [c]Methanol, piperidine, reflux 12 h. [d]NBS, AIBN, DCA, reflux 6 h. [e]CaCO3, H2O, ṉdioxane, 80 °C, 24 h. [f]THF, thioacetic acid, DIPEA, rt, 12 h. [g]The IC_{50} values are the means from at least three independent experiments ($n = 3$). Inactive at 200 μM (highest concentration tested). [h]The IC_{50} value is the mean from two experiments ($n = 2$). Inactive at 20 μM (highest concentrations tested). [i]SI HCT-116 = $[IC_{50}(HEK\ 293)]/[IC_{50}(HCT-116)]$.

hybrids were obtained using 7-hydroxycoumarin as the substrate and different acetobromo-sugars (and its deacetylated form), giving rise to compounds 7 (Scheme 5 and Table 5).

2.2. Biochemistry. *2.2.1. Replication Inhibition (Taq-PCR Assays).* Due to the high degree of structural conservation between DNA polymerases and other DNA-related enzymes, PCR can be used in the search for new antitumor agents. The results revealed that analogues **2d** and **3c** showed the best antireplicative activity with IC_{50} values of 20.7 ± 2.10 and 48.25 ± 1.20 μM, respectively (Table 2).

The search for residues involved in enzyme recognition clearly highlights the ester, thioester, and phenolic hydroxyl functionalizations distributed over the coumarin core. For this reason, hydroxyl groups at C-7 and C-8 for derivative **2c** could be a requirement for the protein−ligand interaction. Addition-

Scheme 3. Synthesis of *O*-Alkenylcoumarin Using Alkenyl Halides (Williamson Synthesis). Derivatization of *O*-Alkenylcoumarins through the Formation of Terminal Epoxides


R₁ = H; R₂ = OH
R₁ = OH; R₂ = H
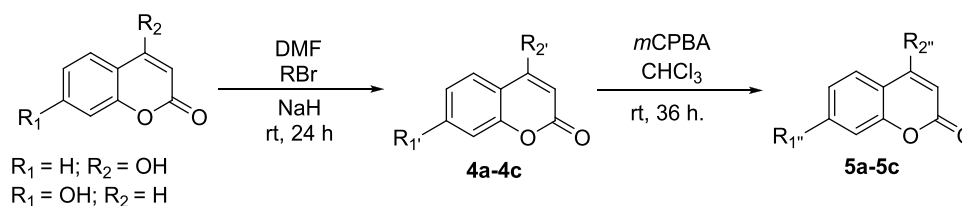
Table 3. Data Collection for RT-MMLV and Growth of Yeast Reporter Strain Inhibition by Compounds 4 and 5

Compound	$R_{1'}$	$R_{2'}$	RT-MMLV IC$_{50}$ Values[a]	Yeast GI$_{50}$ [1;2][b]			
				BY4741	*Δyap1*	*Δrad9 Δrad52*	*SRP-ΔΔΔΔ*
4a	H	*O~~~	>150	>128	>128	>128	>128
4b	*O~~~	H	>150	>128	>128	>128	[105; 55]
4c	*O~~~~	H	>150	[112.1; 130.8]	>128	[>128; 96.3]	[100; 80]
Compound	$R_{1''}$	$R_{2''}$					
5a	H	*O~~~epoxide	>150	>128	>128	[85.5; 71.1]	>128
5b	*O~~epoxide	H	>150	>128	>128	[19.2; 9.7]	[>128; 50]
5c	*O~~~epoxide	H	134.22 ± 2.37	>128	>128	[42.3; 25.2]	>128

[a]The IC$_{50}$ values are the means from at least three independent experiments (*n* = 3). Inactive at 150 μM (highest concentration tested). [b]The GI$_{50}$ values of two independent experiments are shown separated by semicolons. Inactive at 128 μM (highest concentration tested).

Scheme 4. General Procedure of Williamson Reaction

7-hydroxycoumarin　　2e
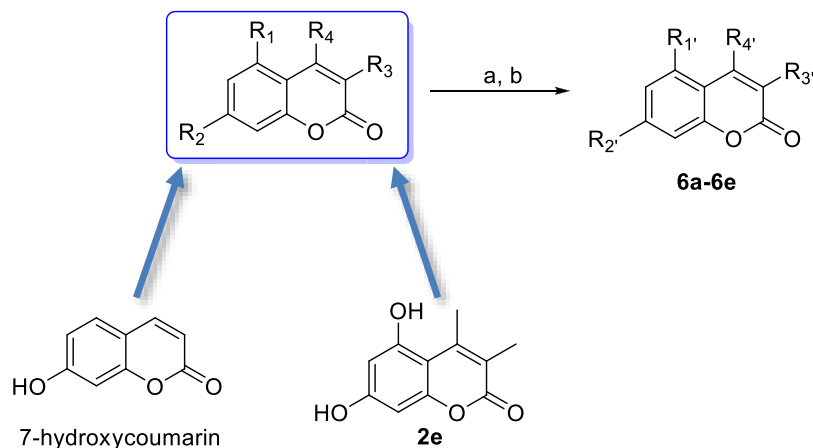
[a]ᵃDMF, NaH, rt, 24 h; ᵇacetone, K₂CO₃, 54 °C, 60 h.

ally, in compound **3c**, the ester group at C-7 and the thioester group on C-4 of the coumarin core have been shown to be important for the protein–ligand–inhibitor complex formation.
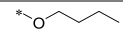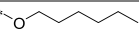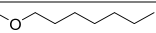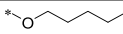
Possibly, such activity consists in the ability to generate hydrogen bonds with the molecular target between H-donor groups through the phenolic hydroxyl for **2c** and acceptor groups such as the ester and thioester groups for **3d**. In addition, obtaining structurally related positional and functional isomers that were shown to be inactive allows us to think that the positions of the mentioned groups on the coumarin nuclei are very important. Apparently, it is a necessary condition that these −OH be present in two positions of the aromatic ring, considering that the monohydroxy derivative of coumarin turned out to be inactive.

Out of four structurally related coumarins (**2a**, **2b**, **2c**, and **2d**), only **2c** and **2d** (both with two hydroxyls on the benzene ring) were active, with IC$_{50}$ values of 142.0 ± 3.40 and 20.7 ± 2.10 μM, respectively, highlighting the importance of the hydroxyl groups on C-7 of the aromatic ring (present in both active derivatives) and C-5. Derivatives with only one −OH group (either in C-6 or C-7) did not show inhibitory activity.

On the other hand, among the esterified and thioesterified coumarin series (**3c**, **3d**, **3e**, **3f**, and **3g**), three of them (**3c**, **3d**, and **3e**) have shown inhibitory activity against *Taq* DNA polymerase with IC$_{50}$ values of 188.35 ± 19.40 μM (**3e**), 143.25 ± 4.22 μM (**3d**), and 48.25 ± 1.20 μM (**3c**). Based on the results obtained for this series (Table 2), it can be observed that the position of the functional group in the aromatic ring is highly relevant. This becomes evident in the IC$_{50}$ values obtained, allowing us to suppose that the groups located on C-

Table 4. Growth of Yeast Reporter Strain Inhibition by Compounds 6

Compound	$R_{1'}$	$R_{2'}$	$R_{3'}$	$R_{4'}$	Yeast GI_{50} [1;2][c]			
					BY4741	Δyap1	Δrad9 Δrad52	SRP-ΔΔΔΔ
[a]6a	H	*—O———	H	H	>128	>128	>128	[105; 100]
[a]6b	H	*—O—————	H	H	>128	>128	>128	[26; 18]
[a]6c	H	*—O——————	H	H	>128	>128	>128	[22; 8]
[b]6d	*—O———I	*—O———I	H	H	>128	>128	>128	>128
[b]6e	*—O————I	*—O————I	H	H	>128	>128	>128	>128
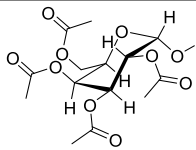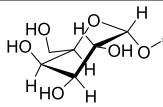
[a]DMF, NaH, rt, 24 h; [b]Acetone, K_2CO_3, 54 °C, 60 h. [c]The GI_{50} values of two independent experiments are shown separated by semicolons. Inactive at 128 μM (highest concentration tested).

Scheme 5. Synthesis of Coumarin-Glucopyranoside Hybrids
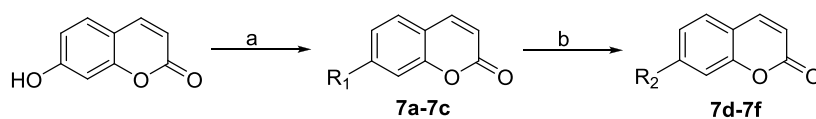
[a]aCH$_2$Cl$_2$, acetobromo-sugar, KOH solution (10%), TBAB, rt, 1 h; [b]CH$_3$OH, sodium methoxide, reflux, 30 min.

Table 5. Coumarin-Pyranoside Chemical Structures (Compounds 7)

Compound	R_1	Compound	R_2
7a		7d	
7b		7e	
7c		7f	

7 (phenolic −OH and methyl ester) generate a better interaction between derivatives **3c** and **3d** over the target. The change in the position of the groups mentioned ab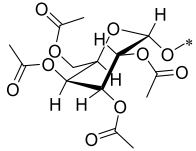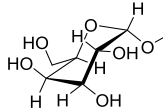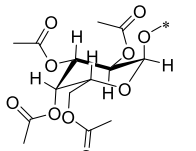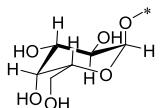ove toward C-6 notably reduces the inhibitory activity of derivatives **3g** (without activity) and **3e** (Table 2). Additionally, the change in functionalization (incorporation of a methoxyl group) on the same oxygen of C-6 in derivative **3f** generates the absence of activity against the DNA *Taq* polymerase enzyme.

2.2.2. Cell Line Assays HCT-116/HEK 293. The antiproliferative effects of the entire coumarin collection were evaluated over HCT-116 (colorectal cancer cell line) and HEK 293 (human embryonic kidney) cell lines. The results showed that derivative **2c** containing the catechol group (C-7 and C-8 of the benzene ring) and a chloromethyl fragment (C-4 of the lactone ring) turned out to be a promising cytotoxic agent against the two cell lines used, showing the greatest cytotoxic effect toward the HCT-116 cell line with an IC_{50} value of 10.08 μM (Figure 1A and Table 2).

Furthermore, due to the fluorescent properties of coumarin nuclei, the internalization of **2c** (CLogP value: 1.776) within the cell through the lipid cell membrane could be verified through fluorescence microscopy monitoring. No preference for location within cell organelles was observed since the presence of **2c** can be noticed throughout the entire cytoplasm (Figure 1B and Figure S115).

Other authors have found that catechols (o-dihydroxybenzene) contain a "free" hydroxyl group (reactive −OH) with a strong hydrogen bond donor with properties similar to those of strongly acidic phenols and an intramolecular H-bonded hydroxyl group (unreactive due to steric protection of the OH group by solvent).[22,23] This effect is not observed in other

A)

B)
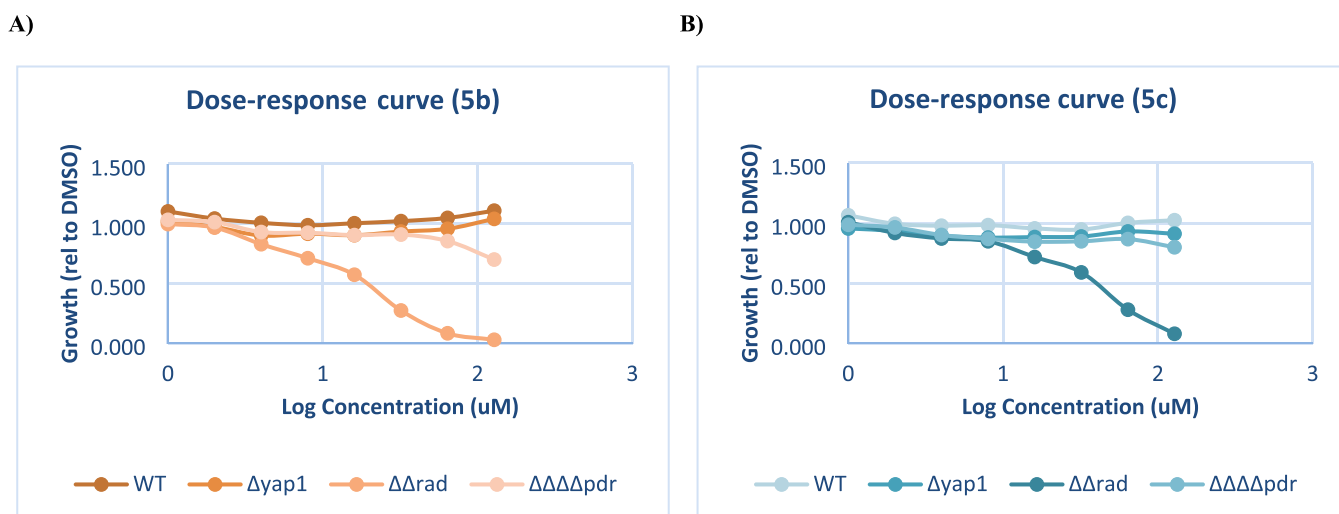
Figure 2. (A) Effect of coumarin derivatives **5b** on the growth of yeast reporter strains. (B) Effect of coumarin derivatives **5c** on the growth of yeast reporter strains. Derivative **5a** showed an inhibition value of ∼78 μM (mean) on Δ*rad9* Δ*rad52*. **5b** and **5c** showed ∼15 μM (mean) and ∼34 μM (mean) on Δ*rad9* Δ*rad52*, respectively, as the most promising compounds.

phenolic compounds such as **2a** and **2b**, and the resorcinol structure (1,3-isomer) of **2d** (CLogP value: 1.706) showing no activity.

These variations in the antiproliferative activity in cells for this series of coumarins (**2a**, **2b**, **2c**, and **2d**) could be attributed to the presence or absence of the catechol group on the benzene ring of coumarin, increasing the hydrophobicity and, therefore, its bioavailability within the cell for compound **2c**.

Finally, the antiproliferative effects shown at the cellular and enzymatic levels (*Taq* DNA polymerase) of **2c** (IC$_{50}$ value: 142.0 ± 3.40 μM), highlighting the selectivity of **2c** (SI HCT-116 = 1.87) on HCT-116 in relation to non-tumor somatic cells, place this compound as a possible pharmacophore as a scaffold for the development of new and better coumarin derivatives with antitumor activity.

2.2.3. Yeast Assay for Common Modes of Action. We also included in this work a determination of comparative growth inhibition in several strains of the yeast *S. cerevisiae* to infer common modes of action and metabolization through chemical−genetic interaction profiles. The growth inhibition was quantitated by means of GI$_{50}$ in dose−response curves.

Based on the abovementioned results, our compounds are predicted to inhibit polymerases. Inhibition of replicative polymerases ends up creating DNA damage, which ultimately leads to cell cycle arrest and cell death. Eukaryotic cells counteract DNA damage through a conserved protein network referred to as the DNA damage response.[24] We made used of the yeast *S. cerevisiae* to test which compounds were cytotoxic in a cell-based *in vivo* assay and whether such compounds were generating DNA damage in the first place. In yeast, Rad9 and Rad52 are at the core of the DNA damage response, and mutants for their genes (Δ*rad9* Δ*rad52* (ΔΔrad)) are hypersensitive to DNA damage relative to a wild-type strain.[25] In addition, the most common mode of action of xenobiotics is oxidative stress, which can also damage DNA as a secondary effect. Yeast cells counteract oxidative stress through the oxidative stress response, in which Yap1 is a key upregulator.[26] Thus, the Δ*yap1* strain is hypersensitive to compounds that primarily elicit oxidative stress. We used this logic to discriminate between direct and secondary DNA damage.

In the reference wild-type strain BY4741, only two compounds showed moderate cytotoxicity, **3f** and **3g** (Table 3). Cytotoxicity was observed for three more compounds in ΔΔrad, **5a**, **5b**, and **5c**, strongly pointing to DNA damage as their mode of action. The relative potency was **5b** > **5c** > **5a**, with no compound showing cytotoxicity in the *yap1*Δ, which rules out DNA damage as a secondary off-target effect of oxidative stress (Figure 3). This was not the case of **3f** and **3g**, in which the increase of cytotoxicity in the ΔΔrad strain relative to the wild type was rather modest and equivalent to that of the Δ*yap1* mutant.

Because the number of cytotoxic compounds in the wild type was low, 2 out of 35, we also tested a strain that is largely defective in the pleotropic drug resistance (ΔΔΔΔpdr). We hypothesized that a bunch of putative cytotoxic compounds were masked by the strong resistance of *S. cerevisiae* to xenobiotics and that with this strain we could increase the number of compounds that could inhibit yeast growth in the 1−128 μM range. The ΔΔΔΔpdr strain is a quadruple knockout mutant for the genes *YOR1*, *YRR1*, *PDR1*, and *PDR3*. *YOR1* encodes an ATP-binding cassette efflux pump, *YRR1* encodes a Zn2-Cys6 zinc-finger transcription factor that is involved in drug resistance, whereas *PDR1* and *PDR3* are paralog genes that encode the major transcription factors that upregulate the expression of multiple genes also implicated in the multidrug resistance. With this strain, eight more compounds were uncovered as cytotoxic **3g**, **6a**, **6b**, **6c**, **7c**, **6f**, **4b**, and **4c**, with **6b** and **6c** being the strongest.

Aside from the cytotoxic studies in yeast, we also tested all compounds against a panel of Gram-positive and Gram-negative bacteria. No compound inhibited bacterial growth in the 1−128 μM range, stressing out their selectivity for eukaryotic cells.

2.2.4. Retrotranscription Inhibition (RT-PCR Assay). On the other hand, we used all compounds obtained to evaluate the reverse transcription process using also a concentration of 250 μM for initial screening. Herein, it could be observed that compound **5c** was active, showing an IC$_{50}$ value of 134.22 ± 2.37 μM (Table 3).

This would indicate that the derivatives obtained from chemical modifications of *O*-alkenylcoumarins (derivatives
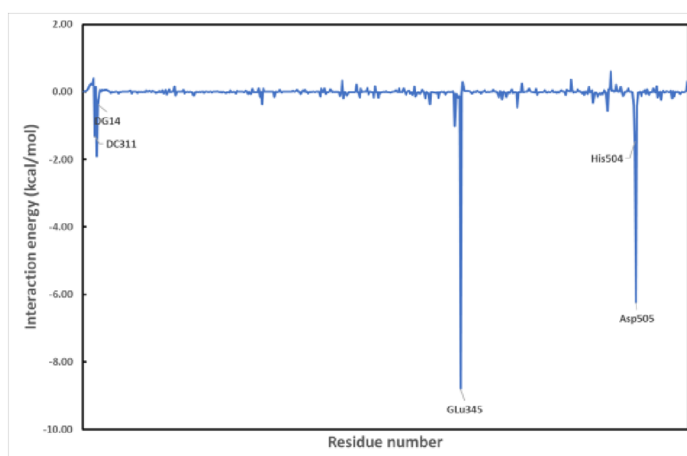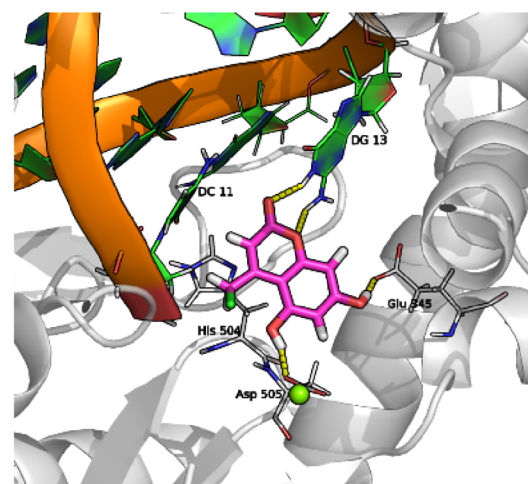
A1)
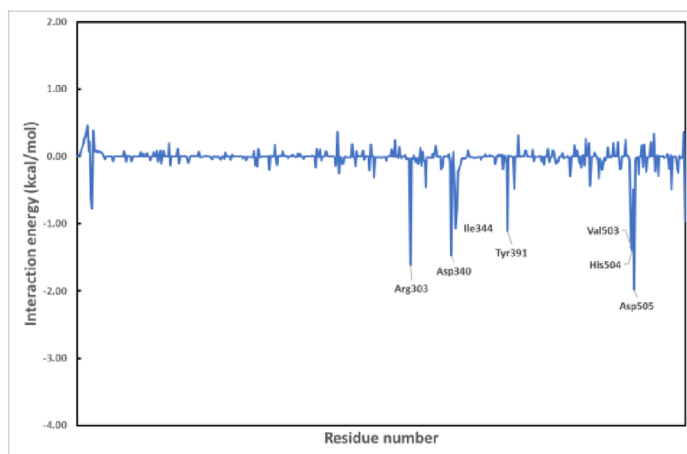
A2)
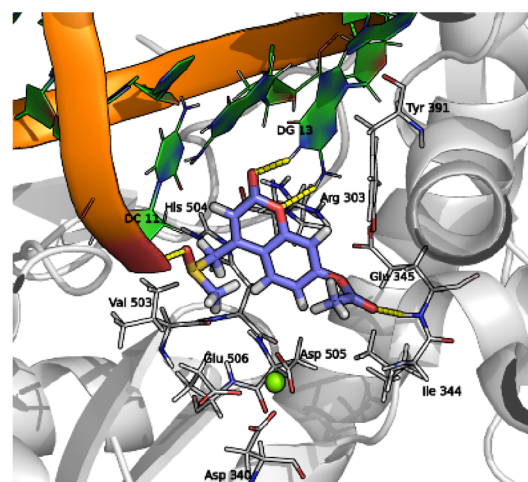
B1)

B2)

Figure 3. Inhibitor/residue and inhibitor/DNA interaction spectra of (A1) polymerase/**3c** and (B1) polymerase/**2d**, according to the MM-GBSA method. The *x*-axis denotes the residue number of *Taq* DNA polymerase I, and the *y*-axis denotes the interaction energy between the inhibitor and specific residues or nucleotides. (A2) Molecular docked complex of **3c** with *Taq* DNA polymerase I [PDB ID: 3RRH]. (B2) Binding pose of coumarin derivative **2d** with the *Taq* DNA polymerase active site.

328 with activity against *Taq* DNA polymerase in a previous
329 research) could be a good starting point for the development
330 of compounds with better antiretroviral and antitumor activity
331 (**5c** also showed activity against Top2 in growth inhibition
332 assays).

333   In this case, the 4,5-epoxypentane functionalization stands
334 out over the derivative containing the 3,4-epoxybutane group
335 (compound **5b** without activity) (Figure 2A,B). Furthermore,
336 the positioning of the mentioned group is of great importance
337 because **5a** (positional isomer on C-4 of the lactone ring of **5c**)
338 did not show activity.

339   **2.3. Computational Studies.** *2.3.1. Computational*
340 *Analysis Based on Protein−Ligand Docking and Molecular*
341 *Dynamics.* To elucidate the interactions in the formation of
342 the protein−DNA polymerase−inhibitor complex, *in silico*
343 simulations (docking and molecular dynamics) of the two best
344 inhibitors were carried out (**3c** and **2d**).

345   All compounds were blind docked with the complete
346 Klentaq DNA polymerase structure using "random seed"
347 variant (for calculation time reasons). Then, we made a site-

directed study within the active site. Despite the lack of 348
structural homology with the natural polymerase substrates, all 349
compounds tested were located within the catalytic site. Both 350
compounds are located within the enzyme active site 351
interacting with the protein and the DNA strands. At this 352
position, the compounds interfere with the binding of the next 353
nucleotide inhibiting therefore the polymerization. 354

   In this study, binding free energy calculations and 355
decomposition of pairwise free energy on a per-residue basis 356
have been executed to precisely explore the molecular basis for 357
the binding for compounds **3c** and **2d**. Therefore, compound 358
3c showed an estimated total binding free energy (ΔG_{total}) of 359
−23.16 kcal/mol, whereas the value obtained for compound 360
2d was −21.36 kcal/mol, which means that compound **3c** 361
bound tighter to the *Taq*-DNA complex and this should 362
translate into a stronger inhibition. 363

   As can be seen in the per-residue energy decomposition 364
(Figure 3A1,B1), compound **3c** binding implies several 365
interactions with residues: *DC11* (deoxycytidine 11), *DG13* 366
(deoxyadenosine 13), *Arg303* (arginine 303), *Asp340* (aspartic 367

acid 340), *Ile344* (isoleucine 344), *Glu345* (glutamic acid 345), *Tyr391* (tyrosine 391), *Val503* (valine 503), *His504* (histidine 340), and *Asp505* (aspartic acid 505). Among them, it is interesting to highlight hydrogen bonds between the inhibitor and main chain NH of *Glu345* and the NH of the guanine base within residue *DG13* (Table 6). Although energy contribution of each interaction is low, the sum of all provides the observed stability of the complex.

Table 6. Acceptor/Donor Groups Involved in the Target–Inhibitor Complex Sorted by Occupancy Values and Average Distance for Compounds 2d and 3c

compound	donor	acceptor	occupancy (%)	average distance (Å)
2d	L22-O_3H_{04}	Glu 345-O_{E2}	100.00	2.52
	L22-O_4H_{05}	Asp 505-O_{D2}	97.20	2.683
	DG 13-N_1H_1	L22-O_{02}	86.41	2.875
3c	Glu 345-NH	L11-O_{13}	48.05	2.933
	DG 13-N_1H_1	L11-O_{02}	38.66	2.909
	DG 13-N_2H_{21}	L11-O_{01}	25.57	2.918
	DC 11-O_3H_3	L11-O_{04}	10.19	2.799

Otherwise, compound **2d** is mainly stabilized by two high-energy interactions with residues *Glu345* and *Asp505* characterized by hydrogen bonds with high occupancy values (Table 6 and Figure 3B1). As occurs with the other compound, derivative **2d** interacts with nucleic acid through hydrogen bonds.

Based on the results obtained through docking and molecular dynamics and a structural comparison of structurally related compounds, we could infer that the inhibitory activity of derivative **2d** could be due to the presence of the two phenolic hydroxyl groups at C-5 and C-7 of the coumarin aromatic ring, which would allow establishing a good interaction within the protein–ligand complex, mainly with hydrogen bond-type interactions between the −OH donor in C-7 and the −COOH portion of the *Glu345* residue, and the hydrogen bond formed between the phenolic −OH of C-5 and the −COOH portion of the *Asp505* residue, the latter being the most protein–inhibitor significant interaction. This is reinforced when the structure of derivative **2d** is compared with derivatives **2a** and **2b**, which only have a phenolic hydroxyl in their aromatic ring in C-7 and C-6, respectively; they showed low or null *in vitro* activity.

On the other hand, the dihydroxylated derivative **2c** at C-7 and C-8 of the aromatic ring did not present a significant inhibition in PCR assays (142.0 ± 3.40 μM). The absence of an −OH at C-5 probably seems to cause the loss of activity in most of the structurally related derivatives of this series, perhaps due to the loss of the interaction with the *Asp505* residue (second in terms of interaction relevance), which could further stabilize the complex. Furthermore, the intramolecular hydrogen bonds present in the catechol group in this derivative could generate a significant decrease in activity against *Taq* DNA polymerase and the opposite in the case of cytotoxicity activity showed in cell line assays. At the same time, derivative **2d** exhibits DNA interaction through the lactone ring of its backbone, primarily via the oxygen in position 1 of the lactone ring and C=O at C-2 with a template DG residue, reinforcing the stabilization of the protein–ligand–inhibitor complex

(Figure 3B2). In this case, the mechanism of the observed cytotoxicity would not only be due to inhibition of DNA polymerases itself but also by inhibition of amplification through the blockade of the incorporation of new ddNTPs through the interaction of the coumarin scaffold with the natural substrate enzyme (DNA).

For derivative **3c**, the protein–ligand interactions shown were mainly due to the hydrogen bond-type interaction with the −NH region of *Glu345* and the C=O of the methyl ester group in position C-7 of the aromatic ring, which added to the rest of generated hydrophobic interactions allows a good complex energy.

The position and presence of the methyl ester group in C-7 could be decisive for enzyme inhibition, since structurally related derivatives such as **3c**, **3d**, **3e**, and **3g**, which are positional isomers or present slight variations with respect to compound **3c**, have shown decreased inhibitory activity. In the case of derivatives **3d** (hydroxylated derivative at C-7, with an IC_{50} value of 143.25 ± 4.22 μM) and **3e** (IC_{50} value of 188.35 ± 19.40 μM), it is observed that small modifications at the structural level have as a consequence a great modification in terms of inhibitory activity. As for compound **3g** (positional isomer of **3c**), it did not show *in vitro* activity, which would allow us to strengthen the methyl ester group at C-7 of the coumarin aromatic ring as a possible pharmacophore group.

3. CONCLUSIONS

In summary, we designed and synthesized 35 *2H*-chromene derivatives as selective and efficient antiproliferative agents, followed by biological evaluated for them.

Enzymatic assays revealed that compounds **2d** and **3c** exhibited strong antiproliferative activity by inhibitory activity toward *Taq* DNA polymerase. We undertook a number of docking simulations and molecular dynamics to better assess, at the *Taq* DNA polymerase binding site, the effect on binding of the two best derivatives. The positioning of key groups on the coumarin scaffold was analyzed together with a study of the available enzymatic space and the effect generated both by the interaction of the inhibitors with the target and with the enzyme's natural substrate, DNA. Among them, the binding mode of active compound **2d** in *Taq* polymerase indicated that the conserved residue *Glu345* was important for ligand binding through the H-bond interaction type. On the other hand, the binding mode for **3c** showed that the conserved residue *Asp505* was the most determinant for the formation of the protein–ligand–inhibitor complex. Moreover, additional interactions of the inhibitors with the enzyme's natural substrate (**2d** with DNA (DG DNA guanine and DC DNA cytosine)) were observed. In conclusion, based on a reasonable molecular design, we found that there was a clear SAR against *Taq* polymerase.

Cell line assays revealed that compound **2c** exhibited good selectivity inhibitory activity toward HCT-116, more than 1.87-fold inhibition levels regarding to normal somatic cells.

Finally, *O*-epoxycoumarin derivatives (**5a**, **5b**, and **5c**) showed DNA damaging activity through *in vivo* tests with the yeast cell model *S. cerevisiae*, highlighting the 4,5-epoxypentane functionalization in C-7 of the coumarin aromatic ring as a possible pharmacophore group (compound **5c**) with antitumor properties, further emphasizing on compounds **5a** and **5c** as new products that have not been previously described in the literature. All these results could

possibly help in the rational design of novel, efficient, and selective antitumoral compounds in the future.

These findings offer valuable insights for the future advancement of novel compounds with improved antitumor properties. Moreover, the derived compounds hold promise as base structures for the development of new compounds with enhanced antiproliferative activity. Although the results allow us to define conclusions, new and more tests will be necessary to determine all the mechanisms of action involved.

4. MATERIALS AND METHODS

4.1. Chemistry. The commercial reagents used were obtained from Sigma-Aldrich, Alfa Aesar, Merck, and Genbiotech. $CDCl_3$ spectral grade solvents were stored over 3 Å molecular sieves for several days. Thin plate chromatography (TLC) was performed on Merck Silica gel 60 F254 chromatoplates. The mobile phases for TLC were mainly mixtures of n-hexane/ethyl acetate (n-hex/AcOEt) in different proportions, varying in increasing polarities. Column chromatographies were carried out on silica gel Merck 60 (230−400 mesh). Solvents were removed using a rotary evaporator.

The purity and structures of all products were determined using standard physical analysis and ^1H and ^{13}C NMR methods.

Ionization techniques (ESI/EI) confirmed the structure of the obtained compounds by the presence of m/z signals assigned to the corresponding pseudomolecular ions of these compounds. All compounds were isolated in pure form after their purification by silica gel column chromatography.

4.2. Spectroscopic Measurements. The NMR spectra were recorded on a Bruker Avance 400 MHz magnetic resonance spectrometer with a BBO 400 MHz S1 probe. The ^1H NMR spectra are reported in chemical shifts downfield from TMS using the respective residual solvent peak as the internal standard ($CDCl_3$ δ 7.26 ppm, acetone-d_6 δ 2.05 ppm, and DMSO-d_6 δ 2.50 ppm). The ^1H NMR spectra are reported as follows: chemical shift (δ, ppm), multiplicity (s = singlet, d = doublet, t = triplet, q = quartet, dd = doublet of doublets, dt = doublet of triplets, dq = doublet of quartets, m = multiplet), coupling constant (J) in Hz, and integration. The ^{13}C NMR spectra are reported in chemical shifts downfield from TMS using the respective residual solvent peak as the internal standard ($CDCl_3$ δ 77.16 ppm, acetone-d_6 δ 29.84/206.26 ppm, and DMSO-d_6 δ 39.52 ppm).

The mass spectrometers used (both ESI and IE) were the following: Waters SYNAPT XS ion mobility Q-TOF mass spectrometer and THERMO ITQ-900 mass spectrometer with a Thermo Scientific TRACE GC Ultra ion trap.

Optical rotation was measured using a PerkinElmer 341 universal precision general-purpose polarimeter with Na and Hg source lamps and a Glan-Taylor polarizer.

4.2.1. General Procedure for the Synthesis of Hydroxycoumarin Esterification (1a−1c). To the commercial compound 7-hydroxycoumarin (0.61 mmol) dissolved in 10 mL of CH_2Cl_2 were added the fatty acid (1.69 mmol), N,N'-dicyclohexylcarbodiimide (DCC) (3.09 mmol), and 4-dimethylaminopyridine (DMAP) (3.07 mmol). The reaction mixture was subjected to constant stirring for 24 h at rt. Then, the reaction mixture was filtrated and concentrated. Finally, the residue obtained was purified by silica gel chromatography, using mixtures of n-Hex/AcOEt of increasing polarity, affording pure products in good yields (46.2−80.0%).

4.2.1.1. 2-Oxo-2H-chromen-7-yl tetradecanoate (1a). Yield: 80.0%, white amorphous solid; ^1H NMR (400 MHz, $CDCl_3$): δ 7.68 (d, 1H, J = 9.52 Hz, H-4), 7.48 (d, 1H, J = 8.41 Hz, H-5), 7.10 (s, 1H, H-8), 7.04 (d, 1H, J = 8.41 Hz, H-6), 6.39 (d, 1H, J = 9.52 Hz, H-3), 2.59 (t, 2H, H-2′), 1.76 (q, 2H, H-3′), 1.26 (m, 23H, H-4′/H-15′), 0.88 (t, 3H, H-16′); ^{13}C NMR (100.62 MHz, $CDCl_3$): δ 171.76 (C-1′), 160.49 (C-2), 154.88 (C-9), 153.49 (C-7), 142.98 (C-4), 128.64 (C-5), 118.58 (C-6), 116.73 (C-10), 116.19 (C-3), 110.60 (C-8), 34.51 (C-2′), 32.07 (C-14′), 29.80 (C-6′ a C-9′), 29.72 (C-10′ a C-11′), 29.59 (C-12′), 29.50 (C-13′), 29.38 (C-5′), 29.22 (C-4′), 24.95 (C-3′), 22.84 (C-15′), 14.27 (C-16′). EI-MS calcd for $C_{25}H_{35}O_4$ $[M + H]^+$ 401.26, found: 401.28.

4.2.1.2. 2-Oxo-2H-chromen-7-yl stearate (1b). Yield: 75.1%, white amorphous solid; ^1H NMR (400 MHz, $CDCl_3$): δ 7.68 (d, 1H, J = 9.52 Hz, H-4), 7.48 (d, 1H, J = 8.41 Hz, H-5), 7.10 (s, 1H, H-8), 7.04 (d, 1H, J = 8.41, H-6), 6.39 (d, 1H, J = 9.52 Hz, H-3), 2.59 (t, 2H, H-2′), 1.76 (q, 2H, H-3′), 1.28 (m, 28H, H-4′/H-17′), 0.88 (t, 3H, H-18′); ^{13}C NMR (100.62 MHz, $CDCl_3$): δ 171.15 (C-1′), 154.91 (C-2), 153.51 (C-9), 142.96 (C-7), 128.64 (C-4), 118.58 (C-5), 116.73 (C-6), 116.20 (C-10), 110.61 (C-3), 34.52 (C-2′), 32.08 (C-16′), 29.83 (C-8), 29.60 (C-14′), 29.51 (C-6′/C-15′), 29.38 (C-5′), 29.23 (C-4′), 24.96 (C-3′), 22.84 (C-17′), 14.26 (C-18′); EI-MS calcd for $C_{27}H_{40}O_4$ $[M + H]^+$ 428.61, found: 428.27.

4.2.1.3. 2-Oxo-2H-chromen-7-yl oleate (1c). Yield: 46.2%, yellow oil; ^1H NMR (400 MHz, $CDCl_3$): δ 7.68 (d, 1H, J = 9.59 Hz, H-4), 7.47 (d, 1H, J = 8.40 Hz, H-5), 7.10 (s, 1H, H-8), 7.03 (d, 1H, J = 8.48, H-6), 6.38 (d, 1H, J = 9.59 Hz, H-3), 5.35 (t, 1H, H-9′), 5.35 (t, 1H, H-10′), 2.58 (t, 2H, H-2′), 2.03 (br s, 4H, H-8′ and H-11′), 1.76 (q, 2H, H-3′), 1.26 (br s, 20H, H-4′/H-7′ and H-12′/H-17′), 0.88 (t, 3H, H-18′); ^{13}C NMR (100.62 MHz, $CDCl_3$): δ 171.75 (C-1′), 160.50 (C-2), 154.85 (C-9), 153.46 (C-7), 143.00 (C-4), 130.22 (C-10′), 129.82 (C-9′), 128.65 (C-5), 118.58 (C-6), 116.72 (C-10), 116.17 (C-3), 110.58 (C-8), 34.47 (C-2′), 32.04 (C-16′), 29.90 (C-12′), 29.81 (C-7′), 29.66 (C-14′), 29.46 (C-13′), 29.20 (C-5′/C-6′), 29.20 (C-4′/C-6′ and C-15′), 27.37 (C-11′), 27.29 (C-8′), 24.91 (C-3′), 22.82 (C-17′), 14.25 (C-18′); EI-MS calcd for $C_{27}H_{38}O_4$ $[M-C_{10}H_{20}]^+$ 302.37, found: 302.14.

4.2.2. General Procedure for Von Pechmann Synthesis (2a−2g). In a round-bottom flask, the acid used as the solvent was added. Subsequently, phenol and the β-ketoester were added under an Ar gas atmosphere. The mixture was stirred for 2 h, with a reaction temperature in the range of 70−120 °C, depending on the phenol used. Once the reaction was complete, the mixture was cooled to room temperature for 20 min and then cold distilled water (50 mL) was added. After that, the mixture was filtered under reduced pressure using a Büchner funnel. Finally, the reaction product was subjected to purification using silica gel column chromatography, using mixtures of n-Hex/AcOEt of increasing polarity. The target compounds were obtained in appreciable yields (10.0−91.0%).

4.2.2.1. 4-(Chloromethyl)-7-hydroxy-2H-chromen-2-one (2a). Yield: 47.5%, white amorphous solid; ^1H NMR (400 MHz, acetone-d_6): δ 7.72 (d, 1H, J = 8.74 Hz, H-5), 6.90 (d, 1H, J = 8.74, H-6), 6.79 (s, 1H, H-8), 6.40 (s, 1H, H-3), 4.91 (s, 2H, H-1′); ^{13}C NMR (100.62 MHz, acetone-d_6): δ 162.12 (C-2), 160.88 (C-7), 156.82 (C-4), 151.48 (C-9), 127.19 (C-5), 113.72 (C-10), 112.56 (C-3), 110.98 (C-6), 103.62 (C-8),

42.17 (C-1′); ESI-MS calcd for $C_{10}H_7O_3ClNa$ [M + Na]$^+$ 232.9981, found: 232.9985.

4.2.2.2. 4-(Chloromethyl)-6-hydroxy-2H-chromen-2-one (2b). Yield: 17.9%, light yellow amorphous solid; ^{1}H NMR (400 MHz, acetone-d_6): δ 7.24 (d, 1H, J = 9.09 Hz, H-8), 7.23 (s, 1H, H-5), 7.16 (d, 1H, J = 9.09 Hz, H-7), 6.60 (s, 1H, H-3), 4.93 (s, 2H, H-1′); ^{13}C NMR (100.62 MHz, acetone-d_6): δ 160.56 (C-2), 154.60 (C-4), 150.80 (C-6), 148.49 (C-9), 120.92 (C-5), 118.85 (C-8), 118.69 (C-7), 116.83 (C-3), 110.42 (C-5), 42.16 (C-1′); ESI-MS calcd for $C_{10}H_7O_3ClNa$ [M + Na]$^+$ 232.9981, found: 232.9985.

4.2.2.3. 4-(Chloromethyl)-7,8-dihydroxy-2H-chromen-2-one (2c). Yield: 22.4%, light brown amorphous solid; ^{1}H NMR (400 MHz, DMSO-d_6): δ 7.17 (d, 1H, J = 8.71 Hz, H-5), 6.84 (d, 1H, J = 8.71 Hz, H-6), 6.41 (s, 1H, H-3), 4.92 (s, 2H, H-1′); ^{13}C NMR (100.62 MHz, DMSO-d_6): δ 161.16 (C-2), 151.45 (C-4), 149.81 (C-7), 143.73 (C-9), 132.51 (C-8), 115.53 (C-5), 112.37 (C-10), 111.00 (C-6), 110.16 (C-3), 41.53 (C-1′); ESI-MS calcd for $C_{10}H_7O_4Cl$ [M + H]$^+$ 227.0106, found: 226.9921.

4.2.2.4. 4-(Chloromethyl)-5,7-dihydroxy-2H-chromen-2-one (2d). Yield: 91.0%, light brown amorphous solid; ^{1}H NMR (400 MHz, DMSO-d_6): δ 6.28 (d, 1H, J = 2.32 Hz, H-8), 6.21 (d, 1H, J = 2.32 Hz, H-6), 6.19 (s, 1H, H-3), 5.01 (s, 2H, H-1′); ^{13}C NMR (100.62 MHz, DMSO-d_6): δ 161.67 (C-2), 160.26 (C-5), 157.29 (C-7), 156.62 (C-4), 152.19 (C-9), 108.89 (C-3), 99.93 (C-10), 99.38 (C-6), 94.93 (C-8), 45.13 (C-1′); ESI-MS calcd for $C_{10}H_7O_4NaCl$ [M + Na]$^+$ 248.9931, found: 248.9935.

4.2.2.5. 5,7-Dihydroxy-3,4-dimethyl-2H-chromen-2-one (2e). Yield: 74.9%, light pink amorphous solid; ^{1}H NMR (400 MHz, acetone-d_6): δ 6.29 (d, 1H, J = 2.14 Hz, H-6), 6.19 (d, 1H, J = 2.14 Hz, H-8), 2.51 (s, 3H, H-2′), 2.00 (s, 3H, H-1′); ^{13}C NMR (100.62 MHz, acetone-d_6): δ 162.22 (C-2), 160.60 (C-5), 157.92 (C-7), 156.10 (C-9), 149.42 (C-4), 116.75 (C-3), 104.06 (C-10), 100.30 (C-6), 95.57 (C-8), 19.33 (C-2′), 12.84 (C-1′); EI-MS calcd for $C_{11}H_{10}O_4$ [M + H]$^+$ 206.05, found: 205.95.

4.2.2.6. 7-Hydroxy-8-methyl-2H-chromen-2-one (2f). Yield: 48.0%, yellow amorphous solid; ^{1}H NMR (400 MHz, CDCl$_3$ + DMSO-d_6): δ 7.50 (d, 1H, J = 9.41 Hz, H-4), 7.02 (d, 1H, J = 8.38 Hz, H-5), 6.71 (d, 1H, H-6), 6.03 (d, 1H, J = 9.41 Hz, H-3), 2.16 (s, 3H, H-1′); ^{13}C NMR (100.62 MHz, CDCl$_3$ + DMSO-d_6): δ 161.82 (C-2), 159.23 (C-7), 153.77 (C-9), 144.23 (C-4), 125.54 (C-5), 112.26 (C-10), 111.98 (C-3), 111.52 (C-6), 111.18 (C-8), 7.82 (C-1′); EI-MS calcd for $C_{10}H_8O_3$ [M + H]$^+$ 176.04, found: 176.17.

4.2.2.7. 4-(Chloromethyl)-6-methoxy-2H-chromen-2-one (2g). Yield: 10.0%, yellow amorphous solid; ^{1}H NMR (400 MHz, CDCl$_3$): δ 7.32 (d, 1H, J = 9.06 Hz, H-8), 7.15 (d, 1H, J = 9.06 Hz, H-7), 7.09 (s, 1H, H-5), 6.58 (s, 1H, H-3), 4.65 (s, 2H, H-2′), 3.88 (s, 3H, H-1′); ^{13}C NMR (100.62 MHz, CDCl$_3$): δ 160.54 (C-2), 156.57 (C-6), 149.22 (C-4), 148.43 (C-9), 119.53 (C-8), 118.57 (C-10), 117.88 (C-7), 116.55 (C-3), 107.38 (C-5), 56.08 (C-1′), 41.50 (C-2′); ESI-MS calcd for $C_{11}H_9ClO_3$ [M + Na]$^+$ 247.0138, found: 247.0134.

4.2.3. Procedure for the Synthesis of Methyl 7-Hydroxy-2-oxo-2H-chromene-3-carboxylate (2h). In a reaction flask under an Ar gas atmosphere, 2,4-dihydroxybenzaldehyde (7.10 mmol), dimethyl malonate (7.81 mmol) and piperidine (0.861 mmol) were dissolved in 11 mL of MeOH. The mixture was stirred for 2 h at reflux. After the reaction was complete, the mixture was cooled in an ice bath for 30 min. Subsequently, the solvent was removed on a rotary evaporator. Finally, the solid obtained was subjected to purification by silica gel column chromatography, using a mixture of *n*-Hex/AcOEt (60:40) by isocratic elution, and the pure product was obtained with an appreciable yield.

4.2.3.1. Methyl 7-Hydroxy-2-oxo-2H-chromene-3-carboxylate (2h). Yield: 47.1%, white amorphous solid; ^{1}H NMR (400 MHz, CDCl$_3$ + DMSO-d_6): δ 8.44 (s, 1H, H-4), 7.36 (d, 1H, J = 8.51 Hz, H-5), 6.77 (d, 1H, J = 8.51 Hz, H-6), 6.71 (s, 1H, H-8), 3.82 (s, 3H, H-2′); ^{13}C NMR (100.62 MHz, CDCl$_3$ + DMSO-d_6): δ 164.07 (C-1′), 163.52 (C-7), 157.09 (C-9), 157.00 (C-2), 149.34 (C-5), 130.69 (C-4), 114.07 (C-3), 111.50 (C-6), 110.10 (C-10), 102.12 (C-8), 52.89 (C-2′); ESI-MS calcd for $C_{11}H_8O_5$ [M + Na]$^+$ 243.0269, found: 243.0266.

4.2.4. Synthesis of 8-(Bromomethyl)-2-oxo-2H-chromen-7-yl acetate (3a). In a reaction flask under an Ar gas atmosphere, 8-methyl-2-oxo-2*H*-chromen-7-yl acetate (6.79 mmol) and *N*-bromosuccinimide (8.15 mmol) were reacted with 2,2′-azobis(2-methylpropionitrile) (AIBN) (0.14 mmol), dissolved in 10 mL of 1,2-dichloroethane used as the solvent. The mixture was stirred for 6 h at reflux. Once the reaction was complete, cold distilled water (50 mL) was added to the reaction mixture and it was left stirring for an additional 4 h. Subsequently, the reaction crude obtained was filtered with a Büchner funnel at reduced pressure. Finally, the reaction product was subjected to purification by silica gel column chromatography, using mixtures of *n*-Hex/AcOEt of increasing polarity, affording a pure product in good yield.

4.2.4.1. 8-(Bromomethyl)-2-oxo-2H-chromen-7-yl acetate (3a). Yield: 63.6%, light yellow amorphous solid; ^{1}H NMR (400 MHz, CDCl$_3$): δ 7.68 (d, 1H, J = 9.51 Hz, H-4), 7.45 (d, 1H, J = 8.44 Hz, H-5), 7.10 (d, 1H, J = 8.44 Hz, H-6), 6.41 (d, 1H, J = 9.51 Hz, H-3), 4.65 (s, 2H, H-1′), 2.41 (s, 3H, H-3′); ^{13}C NMR (100.62 MHz, CDCl$_3$): δ 168.41 (C-2), 159.65 (C-2′), 152.45 (C-7), 151.71 (C-8), 143.15 (C-4), 128.41 (C-5), 119.50 (C-9), 118.90 (C-6), 116.93 (C-10), 116.27 (C-3), 21.07 (C-1′), 19.19 (C-3′); EI-MS calcd for $C_{12}H_9BrO_4$ [M + H]$^+$ 297.10, found: 297.94.

4.2.5. Synthesis of 7-Hydroxy-8-(hydroxymethyl)-2H-chromen-2-one (3b). CaCO$_3$ (20 mmol), dissolved in 9.6 mL of distilled H$_2$O, was added to a reaction flask. Subsequently, a solution of 3a (3.93 mmol) dissolved in 9.6 mL of dioxane was added under an Ar gas atmosphere. The mixture was stirred for 24 h at 80 °C. Once the reaction was complete, the mixture was cooled to room temperature for 30 min and then was filtered with a Büchner funnel under reduced pressure. After that, the solvent was removed on a rotary evaporator, and the solid obtained was treated with AcOEt (3 × 25 mL), and the organic phase was treated with HCl (1 M, 2 × 20 mL). Finally, the reaction crude was subjected to purification by silica gel column chromatography, using mixtures of *n*-Hex/AcOEt of increasing polarity, affording a pure product in high yield.

4.2.5.1. 7-Hydroxy-8-(hydroxymethyl)-2H-chromen-2-one (3b). Yield: 79.7%, light yellow amorphous solid; ^{1}H NMR (400 MHz, CDCl$_3$): δ 7.86 (d, 1H, J = 9.46 Hz, H-4), 7.45 (d, 1H, J = 8.53 Hz, H-5), 6.83 (d, 1H, J = 8.53 Hz, H-6), 6.16 (d, 1H, J = 9.46 Hz, H-3), 5.03 (s, 2H, H-1′); ^{13}C NMR (100.62 MHz, CDCl$_3$): δ 178.96 (C-2), 161.15 (C-7), 160.89 (C-9), 153.91 (C-4), 145.13 (C-5), 129.17 (C-8), 113.98 (C-10), 112.66 (C-3), 112.59 (C-6), 56.04 (C-1′); ESI-MS calcd for $C_{10}H_8O_4$ [M + H]$^+$ 192.0423, found: 191.0337.

4.2.6. Procedure for the Synthesis of Hydroxymercapto-methylcoumarin Derivatives (3c–3g). 4-Chloromethyl-7-hydroxycoumarin (0.95 mmol) and thioacetic acid (1.13 mmol) were dissolved in 8 mL of THF (freshly dist.) under an Ar atmosphere. DIPEA (1.13 mmol) was added dropwise, and the solution was stirred for 4 h at rt. Once the reaction was finished, the reaction crude was treated with CH_2Cl_2 (3×25 mL), and the organic phase was washed with distilled H_2O (3×25 mL). After that, the organic phase obtained was dried with anhydrous $MgSO_4$ and filtered and the solvent was removed on a rotary evaporator. Finally, the reaction crude was subjected to purification by silica gel column chromatography, using a mixture of *n*-Hex/AcOEt by isocratic elution. As a result, the compounds were obtained in appreciable yields (10.0–77.8%).

4.2.6.1. 4-((Acetylthio)methyl)-2-oxo-2H-chromen-7-yl acetate (3c). Yield: 10.0%, light orange amorphous solid; ^1H NMR (400 MHz, acetone-d_6): δ 77.78 (d, 1H, J = 8.46 Hz, H-5), 7.17 (s, 1H, H-8), 7.15 (d, 1H, J = 8.46 Hz, H-6), 6.46 (s, 1H, H-3), 4.33 (s, 2H, H-1′), 2.40 (s, 3H, H-5′), 2.31 (s, 3H, H-3′); ^{13}C NMR (100.62 MHz, acetone-d_6): δ 194.19 (C-2′), 169.26 (C-4′), 160.09 (C-2), 155.40 (C-4), 154.48 (C-9), 151.75 (C-7), 126.58 (C-5), 119.16 (C-6), 115.59 (C-3), 111.33 (C-8), 30.30 (C-5′), 29.57 (C-1′), 20.98 (C-3′); ESI-MS calcd for $C_{14}H_{12}O_5S$ [M + Na]$^+$ 315.0303, found: 315.0307.

4.2.6.2. S-((7-Hydroxy-2-oxo-2H-chromen-4-yl)methyl) ethanethioate (3d). Yield: 70.0%, yellow amorphous solid; ^1H NMR (400 MHz, acetone-d_6): δ 9.46 (br s, 1H, OH), 7.61 (d, 1H, J = 8.76 Hz, H-5), 6.87 (d, 1H, J = 8.76 Hz, H-6), 6.77 (s, 1H, H-8), 6.26 (s, 1H, H-3), 4.28 (s, 2H, H-1′), 2.40 (s, 3H, H-3′); ^{13}C NMR (100.62 MHz, acetone-d_6): δ 194.22 (C-2′), 162.09 (C-2), 160.78 (C-7), 156.74 (C-4), 152.43 (C-9), 127.02 (C-5), 113.67 (C-6), 112.36 (C-10), 111.79 (C-3), 103.67 (C-8), 30.27 (C-3′), 29.53 (C-1′); ESI-MS calcd for $C_{12}H_{10}O_4S$ [M + Na]$^+$ 273.0197, found: 273.0202.

4.2.6.3. S-((6-Hydroxy-2-oxo-2H-chromen-4-yl)methyl) ethanethioate (3e). Yield: 24.8%, yellow amorphous solid; ^1H NMR (400 MHz, CDCl$_3$): δ 7.24 (br d, 1H, J = 8.93 Hz, H-8), 7.05 (d, 1H, J = 8.93 Hz, H-7), 6.98 (s, 1H, H-5), 6.49 (s, 1H, H-3), 4.16 (s, 2H, H-1′), 2.41 (s, 3H, H-3′); ^{13}C NMR (100.62 MHz, CDCl$_3$): δ 193.78 (C-2′), 160.66 (C-2), 152.18 (C-4), 150.15 (C-7), 148.41 (C-9), 120.24 (C-10), 118.91 (C-8), 118.70 (C-7), 116.62 (C-3), 109.36 (C-5), 30.52 (C-1′), 29.30 (C-3′); ESI-MS calcd for $C_{12}H_{10}O_4S$ [M + Na]$^+$ 273.0197, found: 273.0191.

4.2.6.4. S-((6-Methoxy-2-oxo-2H-chromen-4-yl)methyl) ethanethioate (3f). Yield: 64.0%, orange amorphous solid; ^1H NMR (400 MHz, CDCl$_3$): δ 7.28 (d, 1H, J = 9.06 Hz, H-8), 7.12 (d, 1H, J = 9.06 Hz, H-7), 7.01 (s, 1H, H-5), 6.48 (s, 1H, H-3), 4.20 (s, 2H, H-1′), 3.85 (s, 3H, H-4′), 2.41 (s, 3H, H-3′); ^{13}C NMR (100.62 MHz, CDCl$_3$): δ 193.65 (C-2′), 160.68 (C-2), 156.24 (C-6), 150.44 (C-4), 148.44 (C-9), 119.63 (C-8), 118.54 (C-7), 116.47 (C-3), 107.14 (C-5), 56.05 (C-1′), 30.45 (C-4′), 29.35 (C-3′); ESI-MS calcd for $C_{13}H_{12}O_4S$ [M + Na]$^+$ 287.0354, found: 287.0355.

4.2.6.5. 4-((Acetylthio)methyl)-2-oxo-2H-chromen-6-yl acetate (3g). Yield: 77.8%, yellow amorphous solid; ^1H NMR (400 MHz, CDCl$_3$): δ 7.36 (d, 1H, J = 8.77 Hz, H-8), 7.30 (s, 1H, H-5), 7.27 (d, 1H, J = 8.77 Hz, H-7), 6.53 (s, 1H, H-3), 4.16 (s, 2H, H-1′), 2.41 (s, 3H, H-3′), 2.34 (s, 3H, H-5′); ^{13}C NMR (100.62 MHz, CDCl$_3$): δ 193.47 (C-2′), 169.40 (C-4′), 160.15 (C-2), 151.44 (C-4), 150.15 (C-9), 146.81 (C-6), 125.78 (C-8), 118.82 (C-10), 118.52 (C-7), 117.02 (C-5), 116.64 (C-3), 30.50 (C-1′), 29.24 (C-3′), 21.20 (C-5′); ESI-MS calcd for $C_{14}H_{12}O_5S$ [M + Na]$^+$ 315.0298, found: 315.0298.

4.2.7. General Procedure for O-Alkylcoumarin Synthesis (4a–4c). In a round-bottom flask, commercial compound hydroxycoumarin (0.926 mmol), NaH (0.15 mmol), and alkenyl halide (2.07 mmol) dissolved in 4 mL of *N,N′*-dimethylformamide (DMF) were added. The mixture was stirred under an Ar gas atmosphere for 24 h at room temperature. The reaction crude was subsequently treated with ethyl ether (3×25 mL), brine solution (3×25 mL) at rt, and distilled H_2O (2×25 mL) at 5 °C. The organic layer was washed with distilled H_2O (3×25 mL) and then dried with anhydrous Na_2SO_4. The vacuum evaporation residue was subjected to purification by silica gel column chromatography, using mixtures of *n*-Hex/AcOEt of increasing polarity, to give the corresponding products **4** in good yields (55.0–85.1%).

4.2.7.1. 4-(Pent-4-en-1-yloxy)-2H-chromen-2-one (4a). Yield: 85.1%, white amorphous solid; ^1H NMR (400 MHz, CDCl$_3$): δ 7.83 (br dd, 1H, H-5), 7.55 (br dd, 1H, H-6), 7.33 (m, 1H, H-7), 5.85 (s, 1H, H-4′), 5.66 (s, 1H, H-3), 5.10 (br d, 2H, H-5′), 4.15 (t, 2H, H-1′), 2.30 (dd, 2H, H-3′); 2.00 (m, 2H, H-2′); ^{13}C NMR (100.62 MHz, CDCl$_3$): δ 162.25 (C-7), 161.21 (C-2), 155.83 (C-10), 143.40 (C-4), 137.33 (C-4′), 128.67 (C-5), 115.48 (C-5′), 112.88 (C-3), 112.37 (C-6), 101.28 (C-8), 67.70 (C-1′), 29.91 (C-3′), 28.01 (C-2′); EI-MS calcd for $C_{14}H_{14}O_3$ [M + H]$^+$ 230.09, found: 230.16; ESI-MS calcd for $C_{14}H_{14}O_3$ [M + Na]$^+$ 253.0838, found: 253.0835.

4.2.7.2. 7-(But-3-en-1-yloxy)-2H-chromen-2-one (4b). Yield: 55.0%, white amorphous solid; ^1H NMR (400 MHz, CDCl$_3$): δ 7.6 (d, 1H, J = 9.5 Hz, H-4), 7.36 (d, 1H, H-6), 6.85 (br s, 1H, H-8), 6.8 (d, 1H, H-5), 6.23 (d, 1H, J = 9.5 Hz, H-3), 5.9 (m, 1H, H-3′), 5.2 (br d, 2H, H-14′), 4.1 (t, 2H, J = 6.66 Hz, H1′), 2.6 (m, 2H, H-2′); ^{13}C NMR (100.62 MHz, CDCl$_3$): δ 162.09 (C-7), 161.20 (C-2), 155.82 (C-10), 143.40 (C-4), 133.76 (C-3′), 133.40 (C-6), 112.92 (C-3), 112.47 (C-5), 101.34 (C-8), 67.71 (C-1′), 33.26 (C-2′); EI-MS calcd for $C_{13}H_{12}O_3$ [M + H]$^+$ 216.07, found: 216.17; ESI-MS calcd for $C_{13}H_{12}O_3$ [M + Na]$^+$ 239.0695, found: 239.0695.

4.2.7.3. 7-(Pent-4-en-1-yloxy)-2H-chromen-2-one (4c). Yield: 60.3%, white amorphous solid; ^1H NMR (400 MHz, CDCl$_3$): δ 7.63 (d, 1H, J = 9.50 Hz, H-4), 7.36 (d, 1H, H-5), 6.85 (d, 1H, H-6), 6.80 (s, 1H, H-8), 6.25 (d, 1H, J = 9.50 Hz, H-3), 5.90 (m, 1H, H-4′), 5.05 (br d, 2H, H-5′), 4.03 (t, 2H, J = 6.50 Hz, H-1′), 2.30 (q, 2H, H-3′); 1.90 (quint, 2H, H-2′); ^{13}C NMR (100.62 MHz, CDCl$_3$): δ 162.25 (C-7), 161.21 (C-2), 155.83 (C-10), 143.40 (C-4), 137.33 (C-4′), 128.67 (C-5), 115.48 (C-5′), 112.88 (C-3), 112.37 (C-6), 101.28 (C-8), 67.70 (C-1′), 29.91 (C-3′), 28.01 (C-2′); EI-MS calcd for $C_{14}H_{14}O_3$ [M + H]$^+$ 230.09, found: 230.15; ESI-MS calcd for $C_{14}H_{14}O_3$ [M + Na]$^+$ 253.0838, found: 253.0833.

4.2.8. General Procedure for Alkenylcoumarin Epoxidation (5a–5c). A solution of the olefin in CH_2Cl_2 (0.02 mmol/mL) was cooled at 0 °C, and *m*CPBA was added (2 equiv). The ice bath was removed and the solution was stirred for 36 h at rt. The reaction mixture was then diluted with CH_2Cl_2, washed with cold aqueous solution of Na_2SO_4 (10%), saturated solution of NaHCO$_3$, H_2O, and brine solution, dried over anhydrous Na_2SO_4, and concentrated to produce the crude epoxide. The organic phase obtained was dried with anhydrous $MgSO_4$ and vacuum filtered, and the solvent was

removed on a rotary evaporator. Finally, the reaction crude was subjected to purification by silica gel column chromatography, using a mixture of n-Hex/AcOEt of increasing polarity, to give the corresponding products in good yields (41.2−76.4%).

4.2.8.1. 4-(3-(Oxiran-2-yl)propoxy)-2H-chromen-2-one **(5a).** Yield: 57.4%, white amorphous solid; $[\alpha]_D^{20}$: −5.2 (c 3.00; acetone); ^{1}H NMR (400 MHz, CDCl_3): δ 77.79 (d, 1H, J = 7.91 Hz, H-5), 7.54 (t, 1H, H-7), 7.30 (d, 1H, H-8), 7.26 (t, 1H, H-6), 5.67 (s, 1H, H-3), 4.18 (m, 2H, H-1′), 3.01 (m, 1H, 4.11 Hz, H-4′), 2.79 (t, 1H, J = 4.46 Hz, H-5′), 2.52 (m, 1H, J = 5.09 Hz, H-5′), 2.08 (m, 2H, H-2′), 1.90 (m, 1H, H-3′), 1.67 (m, 1H, H-3′); ^{13}C NMR (100.62 MHz, CDCl_3): δ 165.64 (C-4), 163.06 (C-2), 153.43 (C-9), 132.53 (C-7), 124.01 (C-5), 123.03 (C-6), 116.91 (C-8), 115.77 (C-10), 90.65 (C-3), 68.87 (C-1′), 51.75 (C-4′), 47.06 (C-5′), 29.13 (C-2′), 25.33 (C-3′); EI-MS calcd for $C_{14}H_{14}O_4$ [M + H]$^+$ 246.08, found: 246.90.

4.2.8.2. 7-(2-(Oxiran-2-yl)ethoxy)-2H-chromen-2-one **(5b).** Yield: 41.2%, white amorphous solid; $[\alpha]_D^{20}$: −4.3 (c 5.00; acetone); ^{1}H NMR (400 MHz, CDCl_3): δ 7.62 (d, 1H, J = 9.43 Hz, H-4), 7.36 (d, 1H, J = 8.47 Hz, H-5), 6.84 (d, 1H, J = 8.47 Hz, H-6), 6.81 (s, 1H, H-8), 6.23 (d, 1H, J = 9.43 Hz, H-3), 4.17 (m, 2H, H-1′), 3.14 (m, 1H, H-3′), 2.84 (t, 1H, H-4′), 2.58 (dd, 1H, H-4′), 2.16 (m, 1H, J = 6.23 Hz, H-2′), 1.90−1.97 (m, 1H, J = 6.23 Hz, H-2′); ^{13}C NMR (100.62 MHz, CDCl_3): δ 162.03 (C-2), 161.28 (C-7), 155.96 (C-9), 143.50 (C-4), 128.93 (C-5), 113.32 (C-3), 112.89 (C-10), 112.80 (C-6), 101.60 (C-8), 65.44 (C-1′), 49.55 (C-3′), 47.24 (C-4′), 32.31 (C-2′); EI-MS calcd for $C_{13}H_{12}O_4$ [M + H]$^+$ 232.07, found: 231.96.

4.2.8.3. 7-(3-(Oxiran-2-yl)propoxy)-2H-chromen-2-one **(5c).** Yield: 76.4%, white amorphous solid; $[\alpha]_D^{20}$: −4.4 (c 5.63; acetone); ^{1}H NMR (400 MHz, CDCl_3): δ 7.6 (d, 1H, J = 9.44 Hz, H-4), 7.33 (d, 1H, J = 8.50 Hz, H-5), 6.8 (d, 1H, J = 8.50 Hz, H-6), 6.76 (s, 1H, H-8), 6.21 (d, 1H, J = 9.44 Hz, H-3), 4.04 (m, 2H, H-1′), 2.97 (m, 1H, H-4′), 2.76 (t, 1H, H-5′), 2.49 (m, 1H, H-5′), 1.96 (m, 2H, H-2′), 1.81 (m, 1H, H-3′), 1.62 (m, 1H, H-3′); ^{13}C NMR (100.62 MHz, CDCl_3): δ 162.21 (C-2), 161.28 (C-7), 155.94 (C-9), 143.52 (C-4), 128.87 (C-5), 113.11 (C-3), 112.90 (C-10), 112.61 (C-6), 101.46 (C-8), 68.04 (C-1′), 51.88 (C-4′), 47.05 (C-5′), 29.10 (C-3′), 25.67 (C-2′); EI-MS calcd for $C_{14}H_{14}O_4$ [M + H]$^+$ 246.26, found: 246.98.

4.2.9. General Procedure of Coumarin Derivatization Using the Williamson Reaction **(6a−6c).** Hydroxycoumarin (0.926 mmol) was separately dissolved in 4 mL of DMF with 1.5 equiv of NaH and 1 equiv of the used alkyl bromide. The reaction mixture was stirred at room temperature for 24 h. The reaction product was treated with diethyl ether and with brine solution at rt. Then, the organic layer was washed several times with distilled water and then dried with anhydrous Na_2SO_4. The vacuum evaporation residue was purified by silica gel column chromatography, using n-Hex/AcOEt mixtures at increasing polarities, affording pure products in appreciable yields (24.2−63.8%).

4.2.9.1. 7-Butoxy-2H-chromen-2-one **(6a).** Yield: 63.8%, white amorphous solid; ^{1}H NMR (400 MHz, CDCl_3): δ 7.61 (d, 1H, J = 9.53 Hz, H-4), 7.33 (d, 1H, J = 8.62 Hz, H-5), 6.79 (d, 1H, J = 8.62 Hz, H-6), 6.76 (s, 1H, H-8), 6.20 (d, 1H, J = 9.53 Hz, H-3), 3.99 (t, 2H, H-1′), 1.76 (quint, 2H, H-2′), 1.47 (m, 2H, H-3′), 0.95 (t, 3H, H-4′); ^{13}C NMR (100.62 MHz, CDCl_3): δ 162.49 (C-2), 161.33 (C-7), 155.96 (C-9), 143.55 (C-4), 128.78 (C-5), 112.99 (C-3), 112.90 (C-10), 112.41 (C-

6), 101.37 (C-8), 68.39 (C-1′), 31.05 (C-2′), 19.22 (C-3′), 13.84 (C-4′); EI-MS calcd for $C_{13}H_{14}O_3$ [M + H]$^+$ 218.09, found: 217.92.

4.2.9.2. 7-(Hexyloxy)-2H-chromen-2-one **(6b).** Yield: 24.2%, white amorphous solid; ^{1}H NMR (400 MHz, CDCl_3): δ 7.63 (d, 1H, J = 9.43 Hz, H-4), 7.35 (d, 1H, J = 8.53 Hz, H-5), 6.83 (d, 1H, J = 8.53 Hz, H-6), 6.80 (s, 1H, H-8), 6.24 (d, 1H, J = 9.43 Hz, H-3), 4.01 (t, 2H, H-1′), 1.81 (quint, 2H, H-2′), 1.47 (m, 2H, H-3′), 1.34 (m, 2H, H-4′), 1.34 (m, 2H, H-5′), 0.91 (t, 3H, H-6′); ^{13}C NMR (100.62 MHz, CDCl_3): δ 162.60 (C-2), 161.45 (C-7), 156.08 (C-9), 143.59 (C-4), 128.82 (C-5), 113.16 (C-3), 113.06 (C-10), 112.50 (C-6), 101.47 (C-8), 68.82 (C-1′), 31.66 (C-2′), 29.08 (C-3′), 25.77 (C-4′), 22.71 (C-5′); 14.15 (C-6′); EI-MS calcd for $C_{13}H_{18}O_3$ [M + H]$^+$ 246.12, found: 245.95.

4.2.9.3. 7-(Heptyloxy)-2H-chromen-2-one **(6c).** Yield: 40.5%, white amorphous solid; ^{1}H NMR (400 MHz, CDCl_3): δ 7.61 (d, 1H, J = 8.44 Hz, H-4), 7.34 (d, 1H, J = 8.56 Hz, H-5), 6.81 (d, 1H, J = 8.56 Hz, H-6), 6.78 (s, 1H, H-8), 6.22 (d, 1H, J = 8.44 Hz, H-3), 4.00 (t, 2H, H-1′), 1.80 (quint, 2H, H-2′), 1.44 (quint, 2H, H-3′), 1.31 (m, 2H, H-6′), 1.29 (m, 2H, H-5′), 1.29 (m, 2H, H-4′), 0.89 (t, 3H, H-7′); ^{13}C NMR (100.62 MHz, CDCl_3): δ 162.57 (C-2), 161.41 (C-7), 156.05 (C-9), 143.58 (C-4), 128.85 (C-5), 113.11 (C-3), 113.01 (C-10), 112.48 (C-6), 101.45 (C-8), 68.80 (C-1′), 31.85 (C-2′), 29.11 (C-3′), 29.09 (C-4′), 26.03 (C-5′); 22.7 (C-6′), 14.19 (C-7′); EI-MS calcd for $C_{16}H_{20}O_3$ [M + H]$^+$ 260.14, found: 260.02.

4.2.10. General Experimental Procedure for the William-son Reaction **(6d−6e).** Dihydroxycoumarin as the reaction substrate was added to a reaction flask under an Ar gas atmosphere and dissolved in acetone. Then, K_2CO_3 and the corresponding alkyl halide were added. The reaction mixture was stirred for 60 h at 54 °C. Once the reaction was complete, it was cooled to room temperature for 20 min and then the reaction mixture was transferred to a separating funnel. Subsequently, the reaction crude was extracted using CH_2Cl_2 (2 × 10 mL) and then the organic phase obtained was washed with 2 N NaOH solution (3 × 25 mL) and with cold distilled H_2O (3 × 25 mL). The reaction crude was dried with anhydrous $MgSO_4$ and filtered under vacuum and the solvent was removed on a rotary evaporator. Finally, the obtained crude was subjected to purification by silica gel column chromatography, using a mixture of n-Hex/AcOEt (95:5) by isocratic elution. As a result, pure products were obtained with appreciable yields (35.0−47.8%).

4.2.10.1. 4-(Chloromethyl)-5,7-bis(4-iodobutoxy)-2H-chromen-2-one **(6d).** Yield: 35.0%, light yellow amorphous solid; ^{1}H NMR (400 MHz, CDCl_3): δ 6.39 (s, 1H, H-6), 6.26 (s, 1H, H-8), 4.00 (m, 4H, H-1″/H-1‴), 3.25 (m, 4H, H-4″/H-4‴), 2.56 (s, 3H, H-2′), 2.15 (s, 3H, H-1′), 2.02 (m, 6H, H-2″/H-3″/H-3‴), 1.92 (m, 2H, H-2‴); ^{13}C NMR (100.62 MHz, CDCl_3): δ 162.25 (C-2), 160.82 (C-7), 157.91 (C-5), 155.16 (C-9), 148.33 (C-4), 118.07 (C-3), 105.60 (C-10), 96.58 (C-6), 93.76 (C-8), 67.93 (C-1″), 67.21 (C-1‴), 30.33 (C-2″), 30.23 (C-2‴), 30.12 (C-3″), 30.09 (C-3‴), 20.00 (C-2′), 13.17 (C-1′), 6.15 (C-4″), 5.94 (C-4‴); EI-MS calcd for $C_{19}H_{23}I_2O_4$ [M − I]$^+$ 442.06, found: 442.12.

4.2.10.2. 4-(Chloromethyl)-5,7-bis((5-iodopentyl)oxy)-2H-chromen-2-one **(6e).** Yield: 47.8%, yellow oil; ^{1}H NMR (400 MHz, CDCl_3): δ 6.37 (s, 1H, H-8), 6.26 (s, 1H, H-6), 3.98 (m, 4H, H-1″/H-1‴), 3.22 (m, 4H, H-5″/H-5‴), 2.56 (s, 3H, H-2′), 2.13 (s, 3H, H-1′), 1.88 (m, 6H, H-2″/H-4″/H-4‴), 1.82

(m, 2H, H-2″′), 1.61 (m, 4H, H-3″′/H-3″′); ¹³C NMR (100.62 MHz, CDCl₃): δ 162.26 (C-2), 160.91 (C-7), 157.98 (C-8), 155.11 (C-9), 148.49 (C-4), 117.80 (C-3), 105.48 (C-10), 96.52 (C-6), 93.63 (C-8), 68.79 (C-1″), 68.04 (C-1″′), 33.22 (C-4″′), 33.08 (C-4″), 28.20 (C-3″′), 28.08 (C-3″), 27.43 (C-2″′), 27.19 (C-2″), 19.96 (C-2′), 13.13 (C-3′), 6.65 (C-5″), 5.62 (C-5″′); EI-MS calcd for $C_{21}H_{28}I_2O_4$ [M + H]⁺ 598.25, found: 598.11.

4.2.11. General Procedure for Coumarin-Pyranoside Obtention (7a−7c).

The glycosylation methods used in the chemistry of benzopyrans are primarily modifications of the Koenigs−Knorr method.[27] CH₂Cl₂ was used as the organic solvent; KOH aqueous solution (10%) was used as the base. The reaction between equivalent amounts of hydroxycoumarin, base, and acetobromoglucose was performed at rt in the presence of an equivalent amount of tetrabutylammonium bromide (TBABr) as the phase-transfer catalyst. Once the reaction was complete, it was cooled to room temperature for 20 min and the mixture was diluted with CHCl₃ (50 mL). Subsequently, the mixture was transferred to a separating funnel and treated successively with saturated NaCl solution (2 × 25 mL), 1 N KOH (2 × 50 mL), and distilled H₂O (2 × 25 mL). Next, the reaction crude is dried with anhydrous MgSO₄ and filtered under vacuum and the solvent was removed on a rotary evaporator. Finally, the crude obtained was subjected to purification by silica gel column chromatography, using a mixture of n-Hex/AcOEt (80:20) by isocratic elution, affording pure products in appreciable yields (18.2−40.6%).

4.2.11.1. (2R,3S,4S,5R,6R)-2-(Acetoxymethyl)-6-((2-oxo-2H-chromen-7-yl)oxy)tetrahydro-2H-pyran-3,4,5-triyl triacetate (7a).

Yield: 40.6%, white amorphous solid; ¹H NMR (400 MHz, CDCl₃): δ 7.63 (d, 1H, H-4), 7.37 (d, 1H, H-5), 6.94 (s, 1H, H-8), 6.88 (d, 1H, J = 8.55 Hz, H-6), 6.26 (d, 1H, J = 9.58 Hz, H-3), 5.47 (m, 2H, H-5′/H-6′), 5.14 (d, 1H, H-1′), 5.12 (m, 1H, H-4′), 4.17 (m, 2H, H-7b′/H-7a′), 4.12 (d, 1H, H-3′), 2.15 (s, 3H, H-9′), 2.06 (s, 3H, H-15′), 2.04 (s, 3H, H-11′), 1.98 (s, 3H, H-13′). ¹³C NMR (100.62 MHz, CDCl₃): δ 170.46 (C=O), 170.20 (C=O), 170.05 (C=O), 169.35 (C=O), 160.66 (C-2), 159.44 (C-9), 155.43 (C-7), 143.12 (C-4), 128.97 (C-5), 114.55 (C-6), 114.42 (C-3), 114.20 (C-10), 104.13 (C-8), 98.90 (C-1′), 71.53 (C-3′), 70.71 (C-5′), 68.41 (C-6′), 66.91 (C-4′), 61.50 (C-7′), 20.73 (C-9′), 20.69 (C-15′), 20.66 (C-11′), 20.58 (C-13′); ESI-MS calcd for $C_{23}H_{24}O_{12}$ [M + Na]⁺ 515.1160, found: 515.1161.

4.2.11.2. (2R,3S,4R,5R,6R)-2-(Acetoxymethyl)-6-((2-oxo-2H-chromen-7-yl)oxy)tetrahydro-2H-pyran-3,4,5-triyl triacetate (7b).

Yield: 24.4%, white amorphous solid; ¹H NMR (400 MHz, CDCl₃): δ 7.64 (d, 1H, J = 9.54 Hz, H-4), 7.39 (d, 1H, J = 8.54 Hz, H-5), 6.88 (s, 1H, H-8), 6.84 (d, 1H, J = 8.54 Hz, H-6), 6.29 (d, 1H, J = 9.54 Hz, H-3), 5.29 (quint, 2H, H-5′/H-6′), 5.17 (m, 2H, H-1′), 5.15 (m, 1H, H-4′) 4.25 (dd, 1H, H-7b′), 4.17 (d, 1H, H-7a′), 3.91 (m, 1H, H-3′), 2.10 (s, 3H, H-9′), 2.05 (s, 3H, H-15′), 2.04 (s, 3H, H-11′), 2.02 (s, 3H, H-13′). ¹³C NMR (100.62 MHz, CDCl₃): δ 170.69−169.34 (C-2), 160.73 (C-2), 159.42 (C-9), 155.49 (C-7), 143.15 (C-4), 129.02 (C-5), 114.66 (C-6), 114.49 (C-3), 114.36 (C-10), 104.10 (C-8), 98.42 (C-1′), 72.65 (C-3′), 72.51 (C-5′), 71.04 (C-6′), 68.19 (C-4′), 61.94 (C-7′), 20.67 (C-9′/C-15′/C-11′/C-13′); ESI-MS calcd for $C_{23}H_{24}O_{12}$ [M + Na]⁺ 515.1160, found: 515.1161.

4.2.11.3. (2S,4R)-2-(Acetoxymethyl)-6-((2-oxo-2H-chromen-7-yl)oxy)tetrahydro-2H-pyran-3,4,5-triyl triacetate (7c).

Yield: 18.2%, white amorphous solid; ¹H NMR (400

MHz, CDCl₃): δ 7.64 (d, 1H, J = 9.58 Hz, H-4), 7.39 (d, 1H, J = 8.50 Hz, H-5), 6.94 (s, 1H, H-8), 6.89 (d, 1H, J = 8.50 Hz, H-6), 6.30 (d, 1H, J = 9.58 Hz, H-3), 5.30 (quint, 2H, H-5′/H-6′), 5.18 (d, 1H, H-1′), 5.17 (m, 1H, H-4′), 4.27 (m, 1H, H-7b′), 4.17 (d, 1H, H-7a′), 3.92 (m, 1H, H-3′), 2.10 (s, 3H, H-9′), 2.05 (s, 3H, H-15′), 2.05 (s, 3H, H-11′), 2.03 (s, 3H, H-13′); ¹³C NMR (100.62 MHz, CDCl₃): δ 170.71−169.35 (C-2), 160.75 (C-2), 159.43 (C-9), 155.50 (C-7), 143.16 (C-4), 129.03 (C-5), 114.67 (C-6), 114.51 (C-3), 114.37 (C-10), 104.11 (C-8), 98.44 (C-1′), 72.66 (C-3′), 72.52 (C-5′), 71.05 (C-6′), 68.20 (C-4′), 61.95 (C-7′), 20.79 (C-15′), 20.71 (C-11′), 20.68 (C-9′/C-13′); ESI-MS calcd for $C_{23}H_{24}O_{12}$ [M + Na]⁺ 515.1160, found: 515.1169.

4.2.12. General Procedure for Coumarin-Pyranoside Obtention (Modified Zemplen Method) (7d−7f).

In a reaction flask, the corresponding coumarin/peracetylglucopyranoside hybrid, sodium methoxide, dissolved in methanol (MeOH) is added under an Ar gas atmosphere. The reaction mixture is left under constant stirring for 3 h at 65 °C. After that, the reaction mixture was cooled to room temperature for 20 min and was filtered under reduced pressure using a Büchner funnel, and repeatedly washed with cold MeOH. Finally, the obtained crude was subjected to purification by silica gel column chromatography, using a mixture of n-Hex/AcOEt (50:50) by isocratic elution, affording pure products in high yields (60.2−97.5%).

4.2.12.1. 7-(((2R,3R,4S,5R,6R)-3,4,5-Trihydroxy-6-(hydroxymethyl)tetrahydro-2H-pyran-2-yl)oxy)-2H-chromen-2-one (7d).

Yield: 97.5%, white amorphous solid; ¹H NMR (400 MHz, DMSO-d₆): δ 7.99 (d, 1H, J = 9.50 Hz, H-4), 7.64 (d, 1H, J = 8.52 Hz, H-5), 7.04 (s, 1H, H-8), 7.00 (d, 1H, J = 8.52 Hz, H-6), 6.31 (d, 1H, J = 9.50 Hz, H-3), 4.98 (d, 1H, H-1′), 3.71 (br s, 1H, H-2′), 3.67 (t, 1H, H-5′), 3.57−3.60 (m, 1H, H-4′), 3.49−3.56 (m, 2H, H-6a′/H-6b′), 3.44 (m, 1H, H-3′); ¹³C NMR (100.62 MHz, DMSO-d₆): δ 160.37 (C-2), 160.31 (C-9), 155.08 (C-7), 144.30 (C-4), 129.47 (C-5), 113.74 (C-6), 113.25 (C-3), 113.13 (C-10), 103.16 (C-1′), 100.65 (C-8), 75.75 (C-5′), 73.25 (C-3′), 70.14 (C-2′), 68.18 (C-4′), 60.45 (C-6′); ESI-MS calcd for $C_{15}H_{16}O_8$ [M + Na]⁺ 347.0738, found: 347.0750.

4.2.12.2. 7-(((2R,3R,4R,5R,6R)-3,4,5-Trihydroxy-6-(hydroxymethyl)tetrahydro-2H-pyran-2-yl)oxy)-2H-chromen-2-one (7e).

Yield: 67.2%, white amorphous solid; ¹H NMR (400 MHz, DMSO-d₆): δ 8.00 (d, 1H, J = 9.48 Hz, H-4), 7.64 (d, 1H, J = 8.52 Hz, H-5), 7.04 (s, 1H, H-8), 7.01 (d, 1H, J = 8.52 Hz, H-6), 6.32 (d, 1H, J = 9.48 Hz, H-3), 5.01 (d, 1H, J = 7.24 Hz, H-1′), 3.69 (d, 1H, H-2′), 3.23−3.48 (m, 4H, H-4′/H-5′/H-6′), 3.16 (t, 1H, H-3′); ¹³C NMR (100.62 MHz, DMSO-d₆): δ 160.29 (C-2), 160.27 (C-9), 155.06 (C-7), 144.29 (C-4), 129.46 (C-5), 113.69 (C-6), 113.30 (C-3), 113.16 (C-10), 103.20 (C-1′), 100.03 (C-8), 77.18 (C-5′), 76.51 (C-3′), 73.16 (C-2′), 69.67 (C-4′), 60.68 (C-6′); ESI-MS calcd for $C_{15}H_{16}O_8$ [M + Na]⁺ 347.0743, found: 347.0751.

4.2.12.3. 7-(((4S,6S)-3,4,5-Trihydroxy-6-(hydroxymethyl)-tetrahydro-2H-pyran-2-yl)oxy)-2H-chromen-2-one (7f).

Yield: 60.2%, white amorphous solid; ¹H NMR (400 MHz, DMSO-d₆): δ 7.99 (d, 1H, J = 8.49 Hz, H-4), 7.64 (d, 1H, J = 12.54 Hz, H-5), 7.04 (br s, 1H, H-8), 7.00 (d, 1H, J = 8.49 Hz, H-6), 6.32 (d, 1H, J = 12.54 Hz, H-3), 5.10 (d, 1H, J = 7.81 Hz, H-1′), 3.68 (d, 1H, J = 10.25 Hz, H-2′), 3.34 (m, 1H, H-5′), 3.28 (m, 2H, H-4′/H-3′), 3.16 (m, 2H, H-6′); ¹³C NMR (100.62 MHz, DMSO-d₆): δ 160.50 (C-2), 160.38 (C-9), 155.17 (C-7), 144.47 (C-4), 129.63 (C-5), 113.86 (C-6),

113.45 (C-3), 113.29 (C-10), 100.38 (C-1′), 100.15 (C-8), 77.26 (C-5′), 76.54 (C-3′), 73.25 (C-2′), 69.78 (C-4′), 60.79 (C-6′); ESI-MS calcd for $C_{15}H_{16}O_8$ [M + Na]$^+$ 347.0743, found: 347.0743.

4.3. Biological Assays. *4.3.1. Cell Culture Preparation.* The antiproliferative potential of the described compounds was carried out using HEK 293 (Human embryonic kidney 293 cells) and HCT-116 (a human colorectal cancer cell line). The HEK 293 cell line was used as non-tumoral control. All cells were incubated at 37 °C in a 5% CO_2 atmosphere and cultured in DMEM media supplemented with 10% fetal bovine serum (FBS), penicillin (10 μg/mL), and streptomycin (100 μg/mL).[28]

4.3.2. Tumoral Cell Proliferation. To evaluate the effect of the different coumarins on cell proliferation, 5×10^3 cells/well were placed on 96-well culture plates and cultured in DMEM 1640 medium, which was supplemented with 10% FBS and 1% antibiotic (penicillin 10 U/mL + streptomycin 10 μg/mL), at 37 °C in a 5% CO_2 atmosphere for 8 h to allow cell attachment. After attachment, different concentrations of the compounds (1, 10, and 100 μM for drug screening and 1, 10, 25, 50, 75, and 100 μM for IC$_{50}$ calculations) were added, and cells were allowed to grow for 36 h. The number of living cells was estimated by the tetrazolium salt reduction method (MTT, Sigma-Aldrich). The amount of formazan dye generated directly correlates with the number of metabolically active cells in the culture. Proliferation was expressed as the percentage of untreated cells.

4.3.3. Statistical Analyses. All the experiments were conducted with independent repetitions three or five times. The statistical program SPSS was used, and the significance of differences between treatments was evaluated using the LSD test at a level of $p \leq 0.05$. Half maximal inhibitory concentration (IC$_{50}$) values were obtained from the absorbance curves as a function of the API concentration by using GraphPad Prism 8 (GraphPad Software, La Jolla, CA, USA).[29]

4.4. Yeast Strains, Growth Conditions, and Dose–Response Curves. We also included in this work a determination of comparative growth inhibition in several strains of the yeast *S. cerevisiae* to infer common modes of action and metabolization through chemical–genetic interaction profiles. The growth inhibition was quantitated by means of GI$_{50}$ in dose–response curves.

In yeast, Rad9 and Rad52 are at the core of the DNA damage response, and mutants for their genes (Δ*rad9* Δ*rad52* (ΔΔ*rad*)) are hypersensitive to DNA damage relative to a wild-type strain.[25] In addition, the most common mode of action of xenobiotics is oxidative stress, which can also damage DNA as a secondary effect. Yeast cells counteract oxidative stress through the oxidative stress response, in which Yap1 is a key upregulator.[26] Thus, the Δ*yap1* strain is hypersensitive to compounds that primarily elicit oxidative stress. We used this logic to discriminate between direct and secondary DNA damage.

Most yeast strains came from the haploid MATa Euroscarf collection of single-knockout mutants for nonessential genes. The reference wild-type strain for this collection was BY4741. The double mutant Δ*rad9* Δ*rad52* (ΔΔ*rad*) and the quadruple mutant Δ*yrs1* Δ*yrr1* Δ*pdr1* Δ*pdr3* (ΔΔΔΔ*pdr*) strains have been reported before.[30,31]

All strains were grown in the rich YPD medium (1%, w/v, yeast extract, 2%, w/v, peptone, and 2%, w/v, dextrose) at 25 °C. Growth was measured as optical density at 620 nm (OD$_{620}$). We followed a broth microdilution assay in 96-well plates for growth inhibition dose–response curves.[32] The concentration range spanned from 1 to 128 μM, with 1:2 serial dilutions. In each assay, drugs were tested together with eight technical replicates of DMSO 1% (v/v), which served as a "concentration 0" control. The inoculum was set at an OD$_{620}$ of 0.001 (∼25,000 cells/mL). The growth was measured at OD$_{620}$ after 24 h of incubation at 25 °C. The concentration that inhibited growth by 50% (GI$_{50}$) was calculated by fitting a four-parametric curve to the experimental data (https://www.aatbio.com/tools/ic50-calculator).

Correct strain genotypes were verified by their unique resistance to antibiotics associated as markers of the corresponding deletion. In addition, yap1D and radDD were double-checked by their specific sensitivity to menadione (oxidative agent) and phleomycin (DNA damaging agent), respectively.

4.5. Molecular Biology Assays and PCR Products Analysis. The assayed compounds were dissolved in DMSO. The PCR master mixture consisted of 40 mM Tris-acetate pH 8.3, 25 mM MgCl$_2$, 4 U of *Taq* DNA polymerase (Sigma-Aldrich), 20 μM each oligonucleotide primer, and 2.5 mM each deoxynucleotide triphosphate (dNTP). Inhibition studies were carried out with varying compound concentrations. For inhibition control, ddATP at a 200 μM concentration was used. All PCRs were done in 20 μL of reaction volumes. To carry out the PCR assays, the constitutive gene of *Yersinia enterocolitica* 16S rDNA was amplified using specific primers.

Thermocycling conditions consisted of 35 cycles of denaturation at 95 °C for 1 min, followed by primer annealing at 56 °C and primer extension at 72 °C for 90 seg. After completion of the reaction, 4 μL of loading buffer 10× were added. The amplified DNA sequences were electrophoresed for 60 min in 1% agarose gel in buffer TBE 1× (Tris-boric-EDTA, pH 8) at 80−85 V using TBE running buffer 1×. Finally, gels were stained using GelRed Nucleic Acid Gel Stain (Sigma-Aldrich). Amplified DNA bands were detected visually with a UV transilluminator. Each assay was replicated between four times.

4.5.1. Analysis of PCR Products. The relative intensities of GelRed-stained PCR products were analyzed by using the optical scanner and the image program. The image of stained agarose gels was captured using a Photodocumentator UVP Imaging System. The digitized band images were processed using the Image processing program (Scion Image, public domain program), and the IC$_{50}$ values were determined by the GraphPad Prism program.

4.6. In Silico Studies. *4.6.1. Taq DNA Polymerase Model.* The three-dimensional crystal structure of *Taq* DNA polymerase I and Klentaq polymerase employed in this work were obtained from the Protein Data Bank ID code 3RHH. These structures were subjected to energy minimization calculations to remove possible bumps using the Amber12 package.

4.6.2. Docking Simulations. All compounds were blind docked with the complete Klentaq DNA polymerase structure using the "random seed" variant (for calculation time reasons). Then, we made a site-directed study within the active site. Despite the lack of structural homology with the natural polymerase substrates, all compounds tested were located within the catalytic site. Both compounds are located within the enzyme active site interacting with the protein and the DNA strands. At this position, the compounds interfere with

the binding of the next nucleotide inhibiting therefore the polymerization.

Binding free energy calculations and decomposition of pairwise free energy on a per-residue basis for compounds **3c** and **2d** were executed.

Docking simulations were carried out using AutoDock 4.2.[33] In docking experiments, the following parameters were used: the initial population of trial ligands was constituted by 250 individuals and the maximum number of generations was set to 270,000. The maximum number of energy evaluations was 10.0×10^6. All other run parameters were maintained at their default setting. The 3D affinity map was a cube with $50 \times 60 \times 80$ points separated by 0.375 Å and centered on the ddCTP molecule. The resulting docked conformations were clustered into families by the backbone RMSD.

4.6.3. Molecular Dynamics. Molecular dynamics simulations and subsequent structural analysis were performed with the Amber12 package. This was used to describe the complexes, whereas the water molecules were represented by using the TIP3P model. Each model was soaked in a truncated octahedral periodic box of TIP3P water molecules. The distance between the edges of the water box and the closest atom of the solutes was at least 10 Å. Sodium ions were added to neutralize the charge of the system. The entire system was subject to energy minimization in two stages to remove poor contacts between the complex and the solvent molecules. First, the water molecules were minimized by keeping the solute fixed with harmonic constraint with a force of 100 kcal/molÅ². Second, conjugate gradient energy minimizations were performed four times using the positional restraints to all heavy atoms of the complexes with 15, 10, 5, and 0 kcal/molÅ². The values of RMSD between the initial and minimized structures were lower than 0.5 Å. In the next place, each system was then heated in the NVT ensemble from 0 to 300 K in 500 ps and equilibrated at an isothermal isobaric (NPT) ensemble for another 500 ps. A Langevin thermostat[34] was used for temperature coupling with a collision frequency of 1.0 ps⁻¹. The particle mesh Ewald method was employed to treat the long-range electrostatic interactions in a periodic boundary condition. The SHAKE method was used to constrain hydrogen atoms. The time step for all MD is 2 fs, with a direct-space, non-bonded cutoff of 8 Å. Finally, the production was carried out at the NPT conditions performing simulations of 30 ns in length for each system. The interactions between inhibitors and each residue of *Taq* DNA polymerase were calculated using the MM/GBSA decomposition program implemented in AMBER 12.

4.6.3.1. Inhibitor-Residue Interaction Decomposition. The interaction between inhibitor-residue pairs is approximated by

$$\Delta G_{\text{Inhibitor}-\text{residue}} = \Delta G_{\text{vdw}} + \Delta G_{\text{ele}} + \Delta G_{\text{GB}} + \Delta G_{\text{SA}}$$

where ΔG_{vdw} and ΔG_{ele} are non-bonded van der Waals interactions and electrostatic interactions between the inhibitor and each *Taq* DNA polymerase I residue in the gas phase. The polar contribution to solvation free energy (ΔG_{GB}) was calculated by using the GB module. ΔG_{SA} is the free energy due to the solvation process of nonpolar contribution and was calculated from SASA. All energy components in the equation were calculated using 500 snapshots from the last 5 ns of the MD simulation.

4.7. RT-PCR Assays. Total RNA was extracted using Trizol (Invitrogen, Waltham, MA) according to the manufacturer's instructions. The purity and concentration of the samples were checked measuring the absorbance at 260 and 280 nm using a NanoQuant microplate reader (BioTek, Epoch, Vermont). Only RNA samples with an Abs260/Abs280 ratio between 1·8 and 2·0 were used for gene expression analyses. Retrotranscription was carried out with M-MLV Reverse Transcriptase virus enzyme 200 U μL^{-1} (Sigma-Aldrich) according to the manufacturer's instructions. Two micrograms of isolated RNA, previously suspended in diethylpyrocarbonate-treated water, was used. The primer design was done using PubMed database and OligoCalc software. The gene expression levels were normalized to the levels of the 16S rRNA housekeeping gene utilizing ImageJ 1.51n software for relative quantification.[35]

After completion of the reaction, 4 μL of loading buffer 10× was added. The amplified DNA sequences were electrophoresed for 60 min in 1% agarose gel in buffer TBE 1× (Tris-boric-EDTA, pH 8) at 80−85 V using TBE running buffer 1×. Finally, gels were stained using GelRed Nucleic Acid Gel Stain (Sigma-Aldrich). For inhibition control, ddATP at 200 μM concentration was used. Amplified DNA bands were detected visually with a UV transilluminator. Each assay was replicated between four times.

4.7.1. Analysis of RT-PCR Products. The relative intensities of GelRed-stained RT-PCR products were analyzed by using the optical scanner and the image program. The image of stained agarose gels was captured using a Photodocumentator UVP Imaging System. The digitized band images were processed using the Image processing program (Scion Image, public domain program), and the IC$_{50}$ values were determined by the GraphPad Prism program.

■ ASSOCIATED CONTENT

Ⓢ Supporting Information

The Supporting Information is available free of charge at https://pubs.acs.org/doi/10.1021/acsomega.3c03181.

■ AUTHOR INFORMATION

Corresponding Author

Ezequiel F. Bruna-Haupt − *National University of San Luis, San Luis 5700, Argentina; Chemical Technology Research Institute-National Council for Scientific and Technical Research (INTEQUI-CONICET), San Luis 5700, Argentina;* ⓞ orcid.org/0000-0003-2644-6935; Email: ezequiel20j33803@gmail.com

Authors

Marcelle D. Perretti − *Institute of Bio-Organics Antonio González, Department of Organic Chemistry, University of La Laguna, Institute of Natural Products and Agrobiology, IPNA-CSIC, La Laguna 38206, Spain*

Hugo A. Garro − *National University of San Luis, San Luis 5700, Argentina; Chemical Technology Research Institute-National Council for Scientific and Technical Research (INTEQUI-CONICET), San Luis 5700, Argentina; Max Planck Laboratory for Structural Biology, Chemistry and Molecular Biophysics of Rosario (MPLbioR, UNR-MPIbpC), and Instituto de Investigaciones para el Descubrimiento de Fármacos de Rosario (IIDEFAR, UNR-CONICET), Rosario S2002LRK, Argentina; National University of Rosario, Rosario, Santa Fe 3100, Argentina*

Romen Carrillo − *Institute of Bio-Organics Antonio González, Department of Organic Chemistry, University of La Laguna, Institute of Natural Products and Agrobiology, IPNA-CSIC, La Laguna 38206, Spain;* orcid.org/0000-0002-7078-300X

Félix Machín − *Research Unit, Nuestra Señora de Candelaria University Hospital, Santa Cruz de Tenerife 38010, Spain, Institute of Biomedical Technologies, University of La Laguna, Tenerife 38200, Spain; Faculty of Health Sciences, Fernando Pessoa Canarias University, Las Palmas de Gran Canaria 35450, Spain*

Isabel Lorenzo-Castrillejo − *Research Unit, Nuestra Señora de Candelaria University Hospital, Santa Cruz de Tenerife 38010, Spain, Institute of Biomedical Technologies, University of La Laguna, Tenerife 38200, Spain*

Lucas Gutiérrez − *National University of San Luis, San Luis 5700, Argentina*

Esteban G. Vega-Hissi − *National University of San Luis, San Luis 5700, Argentina*

Macarena Mamberto − *National University of Rosario, Rosario, Santa Fe 3100, Argentina; Institute of Clinical and Experimental Immunology of Rosario (IDICER; CONICET-UNR), Center for Research and Production of Biological Reagents (CIPReB; FCM-UNR), Faculty of Medical Sciences, Rosario, Santa Fe 3100, Argentina*

Mauricio Menacho-Marquez − *National University of Rosario, Rosario, Santa Fe 3100, Argentina; Institute of Clinical and Experimental Immunology of Rosario (IDICER; CONICET-UNR), Center for Research and Production of Biological Reagents (CIPReB; FCM-UNR), Faculty of Medical Sciences, Rosario, Santa Fe 3100, Argentina*

Claudio O. Fernández − *Max Planck Laboratory for Structural Biology, Chemistry and Molecular Biophysics of Rosario (MPLbioR, UNR-MPIbpC), and Instituto de Investigaciones para el Descubrimiento de Fármacos de Rosario (IIDEFAR, UNR-CONICET), Rosario S2002LRK, Argentina; National University of Rosario, Rosario, Santa Fe 3100, Argentina*

Celina García − *Institute of Bio-Organics Antonio González, Department of Organic Chemistry, University of La Laguna, Institute of Natural Products and Agrobiology, IPNA-CSIC, La Laguna 38206, Spain;* orcid.org/0000-0002-5049-9466

Carlos R. Pungitore − *National University of San Luis, San Luis 5700, Argentina; Chemical Technology Research Institute-National Council for Scientific and Technical Research (INTEQUI-CONICET), San Luis 5700, Argentina*

Complete contact information is available at:
https://pubs.acs.org/10.1021/acsomega.3c03181

Author Contributions

The manuscript was written through contributions of all authors. Conceived the project: C.R.P., H.A.G., and C.G. Performed experiments: E.F.B.-H, M.D.P., F.M., I.L.-C., L.G. E.G.V.-H., M.M., and M.M.-M. Analyzed data: E.F.B.-H., H.A.G., R.C., F.M. M.M.-M., C.O.F., C.G., and C.R.P. Prepared the manuscript: E.F.B.-H., H.A.G, C.G., and C.R.P. All authors have given approval to the final version of the manuscript.

■ REFERENCES

(1) Berdis, A. J. DNA polymerases as therapeutic targets. *Biochemistry* **2008**, *47*, 8253−8260.

(2) Kitao, H.; Limori, M.; Kataoka, Y.; Takeshi, W.; Eriko, T.; Hiroshi, S.; Eiji, O.; Yoshihiko, M. DNA replication stress and cancer chemotherapy. *Cancer Sci.* **2018**, *109*, 264−271.

(3) Maeda, N.; Hada, T.; Yoshida, H.; Mizushina, Y. Inhibitory effect on replicative DNA polymerases, human cancer cell proliferation, and in vivo anti-tumor activity by glycolipids from spinach. *Curr. Med. Chem.* **2007**, *14*, 955−967.

(4) Wang, F.; Ding, N.; Liu, Z.; Ji, Y. Y.; Yue, Z. Ablation damage characteristic and residual strength prediction of carbon fiber/epoxy composite suffered from lightning strike. *Compos. Struct.* **2014**, *117*, 222−233.

(5) Bisi, A.; Cappadone, C.; Rampa, A.; Farruggia, G.; Sargenti, A.; Belluti, F.; Di Martino, R.; Malucelli, E.; Meluzzi, A.; Iotti, S.; Gobbi, S. Coumarin derivatives as potential antitumor agents: Growth inhibition, apoptosis induction and multidrug resistance reverting activity. *Eur. J. Med. Chem.* **2017**, *127*, 577−585.

(6) Zhang, L.; Xu, Z. Coumarin-containing hybrids and their anticancer activities. *Eur. J. Med. Chem.* **2019**, *181*, 111587−111606.

(7) Ren, Q. C.; Gao, C.; Xu, Z.; Feng, L. S.; Liu, M. L.; Wu, X.; Zhao, F. Bis-coumarin Derivatives and Their Biological Activities. *Curr. Top. Med. Chem.* **2018**, *18*, 101−113.

(8) An, R.; Hou, Z.; Li, J. T.; Yu, H. N.; Mou, Y. H.; Guo, C. Design, Synthesis and Biological Evaluation of Novel 4-Substituted Coumarin Derivatives as Antitumor Agents. *Molecules* **2018**, *23*, 2281−2293.

(9) Katsori, A. M.; Hadjipavlou-Litina, D. Coumarin derivatives: an updated patent review (2012-2014). *Expert Opin. Ther. Pat.* **2014**, *24*, 1323−1347.

(10) Lv, N.; Sun, M.; Liu, C.; Li, J. Design and synthesis of 2-phenylpyrimidine coumarin derivatives as anticancer agents. *Bioorg. Med. Chem. Lett.* **2017**, *27*, 4578−4581.

(11) Zhang, L.; Jiang, G.; Yao, F.; He, Y.; Liang, G.; Zhang, Y.; Hu, B.; Wu, Y.; Li, Y.; Liu, H. Growth inhibition and apoptosis induced by osthole, a natural coumarin, in hepatocellular carcinoma. *PLoS One* **2012**, *7*, 37865−37874.

(12) Baghdadi, M. A.; Al-Abbasi, F. A.; El-Halawany, A. M.; Aseeri, A. H.; Al-Abd, A. M. Anticancer Profiling for Coumarins and Related O-Naphthoquinones from Mansonia gagei against Solid Tumor Cells in Vitro. *Molecules* **2018**, *23*, 1020−1033.

(13) Garro, H. A.; Manzur, J. M.; Ciuffo, G. M.; Tonn, C. E.; Pungitore, C. R. Inhibition of reverse transcriptase and Taq DNA

1469 polymerase by compounds possessing the coumarin framework.
1470 *Bioorg. Med. Chem. Lett.* **2014**, *24*, 760−764.

1471 (14) Wang, H.; Xu, W. Mito-methyl coumarin, a novel
1472 mitochondria-targeted drug with great antitumor potential was
1473 synthesized. *Biochem. Biophys. Res. Commun.* **2017**, *489*, 1−7.

1474 (15) Hu, X. L.; Xu, Z.; Liu, M. L.; Feng, L. S.; Zhang, G. D. Recent
1475 Developments of Coumarin Hybrids as Anti-fungal Agents. *Curr. Top.*
1476 *Med. Chem.* **2017**, *17*, 3219−3231.

1477 (16) Xu, Z.; Chen, Q.; Zhang, Y.; Liang, C. Coumarin-based
1478 derivatives with potential anti-HIV activity. *Fitoterapia* **2021**, *150*,
1479 104863−104873.

1480 (17) Bruna-Haupt, E. F.; Garro, H. A.; Gutiérrez, L.; Pungitore, C.
1481 R. Collection of alkenylcoumarin derivatives as Taq DNA polymerase
1482 inhibitors: SAR and in silico simulations. *Med. Chem. Res.* **2018**, *27*,
1483 1432−1442.

1484 (18) Kostova, I. Synthetic and natural coumarins as cytotoxic agents.
1485 *Curr. Med. Chem. Anticancer Agents.* **2005**, *5*, 29−46.

1486 (19) Zhu, J. J.; Jiang, J. G. Pharmacological and Nutritional Effects of
1487 Natural Coumarins and Their Structure-Activity Relationships. *Mol.*
1488 *Nutr. Food Res.* **2018**, *62*, 1−74.

1489 (20) Al-Warhi, T.; Sabt, A.; Elkaeed, E. B.; Eldehna, W. M. Recent
1490 advancements of coumarin-based anticancer agents: An up-to-date
1491 review. *Bioorg. Chem.* **2020**, *103*, 104163−104178.

1492 (21) Zhu, H.; Yu, L.; Liu, J.; Wang, M.; Zhang, T.; Qiu, F. A new
1493 coumarin glucoside ester from seeds oil leavings of *Xanthoceras*
1494 *sorbifolia. Chin. Herb. Med.* **2018**, *11*, 113−115.

1495 (22) Foti, M. C.; Barclay, L. R.; Ingold, K. U. The role of hydrogen
1496 bonding on the h-atom-donating abilities of catechols and
1497 naphthalene diols and on a previously overlooked aspect of their
1498 infrared spectra. *J. Am. Chem. Soc.* **2002**, *124*, 12881−12888.

1499 (23) Ortega-Moo, C.; Garza, J.; Vargas, R. The substituent effect on
1500 the antioxidant capacity of catechols and resorcinols. *Theor. Chem.*
1501 *Acc.* **2016**, *135*, 1−12.

1502 (24) Symington, L. S.; Rothstein, R.; Lisby, M. Mechanisms and
1503 Regulation of Mitotic Recombination in Saccharomyces cerevisiae.
1504 *Genetics* **2014**, *198*, 795−835.

1505 (25) Quintana-Espinoza, P.; García-Luis, J.; Amesty, A.; Martín-
1506 Rodríguez, P.; Lorenzo-Castrillejo, I.; Ravelo, A. G.; Fernández-Pérez,
1507 L.; Machín, F.; Estévez-Braun, A. Synthesis and study of
1508 antiproliferative, antitopoisomerase II, DNA-intercalating and DNA-
1509 damaging activities of arylnaphthalimides. *Bioorg. Med. Chem.* **2013**,
1510 *21*, 6484−6495.

1511 (26) Toone, W. M.; Jones, N. AP-1 transcription factors in yeast.
1512 *Curr. Opin. Genet. Dev.* **1999**, *9*, 55−61.

1513 (27) Koenigs, W.; Knorr, E. Ueber einige Derivate des
1514 Traubenzuckers und der Galactose. *Ber. Dtsch. Chem. Ges.* **2006**, *34*,
1515 957−981.

1516 (28) Garro, H. A.; Bruna-Haupt, E.; Cianchino, V.; Malizia, F.;
1517 Favier, S.; Menacho-Marquez, M.; Cifuente, D.; Fernandez, C. O.;
1518 Pungitore, C. R. Verbascoside, synthetic derivatives and other
1519 glycosides from Argentinian native plant species as potential
1520 antitumoral agents. *Nat. Prod. Res.* **2021**, *35*, 4703−4708.

1521 (29) Priotti, J.; Baglioni, M. V.; García, A.; Rico, M. J.; Leonardi, D.;
1522 Lamas, M. C.; Menacho Márquez, M. Repositioning of Anti-parasitic
1523 Drugs in Cyclodextrin Inclusion Complexes for Treatment of Triple-
1524 Negative Breast Cancer. *AAPS PharmSciTech.* **2018**, *19*, 3734−3741.

1525 (30) Anaissi-Afonso, L.; Oramas-Royo, S.; Ayra-Plasencia, J.;
1526 Martín-Rodríguez, P.; García-Luis, J.; Lorenzo-Castrillejo, I.;
1527 Fernández-Pérez, L.; Estévez-Braun, A.; Machín, F. Lawsone, Juglone,
1528 and *β*-Lapachone Derivatives with Enhanced Mitochondrial-Based
1529 Toxicity. *ACS Chem. Biol.* **2018**, *13*, 1950−1957.

1530 (31) Miyamoto, Y.; Machida, K.; Mizunuma, M.; Emoto, Y.; Sato,
1531 N.; Miyahara, K.; Hirata, D.; Usui, T.; Takahashi, H.; Osada, H.;
1532 Miyakawa, T. Identification of Saccharomyces cerevisiae isoleucyl-
1533 tRNA synthetase as a target of the G1-specific inhibitor Reveromycin
1534 A. *J. Biol. Chem.* **2002**, *277*, 28810−28814.

1535 (32) Ramos-Pérez, C.; Lorenzo-Castrillejo, I.; Quevedo, O.; García-
1536 Luis, J.; Matos-Perdomo, E.; Medina-Coello, C.; Estévez-Braun, A.;
1537 Machín, F. Yeast cytotoxic sensitivity to the antitumour agent *β*-

1538 lapachone depends mainly on oxidative stress and is largely
1539 independent of microtubule- or topoisomerase-mediated DNA
1540 damage. *Biochem. Pharmacol.* **2014**, *92*, 206−219.

1541 (33) Morris, G. M.; Huey, R.; Lindstrom, W.; Sanner, M. F.; Belew,
1542 R. K.; Goodsell, D. S.; Olson, A. J. AutoDock4 and AutoDockTools4:
1543 Automated docking with selective receptor flexibility. *J. Comput.*
1544 *Chem.* **2009**, *30*, 2785−2791.

1545 (34) Larini, L.; Mannella, R.; Leporini, D. Langevin stabilization of
1546 molecular dynamics. *J. Chem. Phys.* **2007**, *126*, 104101−104109.

1547 (35) Estrada, C. S.; Velázquez, L. C.; Escudero, M. E.; Favier, G. I.;
1548 Lazarte, V.; de Guzmán, A. M. S. Pulsed field, PCR ribotyping and
1549 multiplex PCR analysis of Yersinia enterocolitica strains isolated from
1550 meat food in San Luis Argentina. *Food Microbiol.* **2011**, *28*, 21−28.